Mantle Petrology: Field Observations and High Pressure Experimentation: A Tribute to Francis R. (Joe) Boyd
© The Geochemical Society, Special Publication No. 6, 1999
Editors: Yingwei Fei, Constance M. Bertka, and Bjorn O. Mysen

The composition and origin of sub-continental lithospheric mantle

W. L. GRIFFIN,[1,2] SUZANNE Y. O'REILLY,[1] and C. G. RYAN[2]

[1]Key Centre for Geochemical Evolution and Metallogeny of Continents, Macquarie University, NSW 2109, Australia
[2]CSIRO Exploration and Mining, P.O. Box 136, North Ryde, NSW 2113, Australia

Abstract—Data from xenoliths, garnet concentrates and peridotite massifs demonstrate secular evolution in the composition of subcontinental lithospheric mantle (SCLM), related to the age of the last major tectonothermal event in the overlying crust. Equations relating the Cr_2O_3 content of garnets in mantle-derived xenoliths to bulk-rock composition allow calculation of mean SCLM compositions for 28 regions of different crustal age. Subcalcic (cpx-free) garnet harzburgites are restricted to Archean mantle, and the dominant lherzolites become progressively less depleted (in terms of major-element composition) from Archean through Proterozoic to Phanerozoic time. Most Archean SCLM probably was derived by high-degree melting at depths ≥150 km, and no Cr-Al phase was present in the residue. Observed variations in olivine/orthopyroxene ratios may reflect both sorting of olivine and high-T opx, and variable degrees of melt interaction leading to more olivine-rich rocks. Comparison of SCLM xenolith suites with peridotites from convergent-margin settings and ocean basins suggests that accretion of subducted oceanic mantle is not a major process in the production of SCLM. Most existing Proterozoic and Phanerozoic SCLM probably has been generated in extensional environments; typical Phanerozoic SCLM has experienced ≤10% melt extraction, while Proterozoic lithosphere is generally more depleted. The density of mean Archean SCLM is ≈1.5% less than that of mean Phanerozoic SCLM, while Proterozoic SCLM is intermediate in density. Continental roots imaged beneath cratons by seismic tomography reflect compositional differences, reinforced by differences in the mean geotherm between Archean and younger areas. The broad correlation of SCLM composition with crustal age implies quasi-contemporaneous formation of crustal volumes and their underlying SCLM, and crust-mantle coupling over timespans measured in aeons; this coupling is directly related to density. Depleted Archean and Proterozoic SCLM is buoyant relative to asthenosphere even when "cold", and cannot be delaminated by gravitational processes alone. This situation limits the potential for recycling of ancient SCLM, invoked by some isotopic models. However, episodes of continental rifting may mix Archean SCLM with younger more fertile (and hence denser) material, which might eventually be delaminated; this could provide a mechanism for lithosphere recycling.

INTRODUCTION

THE SUBCONTINENTAL lithospheric mantle (SCLM) represents a chemical, thermal and mechanical boundary layer insulating the continental crust from the hotter and more dynamic interior of the Earth. Disruption or removal of this insulating layer by tectonic processes produces changes in the heat budget of the crust, with consequences that include uplift, magmatism, and the formation of large mineral deposits. To understand the behaviour of the SCLM in different tectonic situations, we need data on the lateral, vertical and temporal variations in the composition of the SCLM, and how these variations affect its buoyancy and rheology. For realistic modelling of large-scale geophysical data, we also need to be able to separate the effects of SCLM composition from those of intensive parameters such as temperature and pressure.

Several studies (BOYD and MERTZMAN, 1987; BOYD, 1989, 1997; IONOV *et al.*, 1993; GRIFFIN *et al.*, 1998a) have suggested that SCLM composition is related to tectonic setting, and/or to the age of the SCLM; if this is the case, then a detailed knowledge of SCLM composition can provide significant clues to the evolution of large-scale processes through Earth's history.

This paper will therefore: (1) examine the evidence for temporal changes in the composition of the SCLM; (2) estimate the mean composition of SCLM beneath crustal provinces of different tectonic setting and age; (3) examine the geophysical responses of different types of mantle and the tectonic consequences of changing SCLM composition; (4) speculate on the processes that have created and destroyed SCLM throughout Earth's history.

Much of the SCLM has existed for >1 Ga, and it acts in many respects as a chemical filter paper, "absorbing" material from rising melts and other fluids, so that over time it may become chemically distinct from the rest of Earth's mantle, especially in terms of trace-element abundances and isotopic composition (MENZIES, 1990). Although these changes are important for tracking the long-term evolution of geochemical reservoirs, and elucidating the origin of specific types of magmatic rocks, this paper will not deal with these aspects; it will focus primarily on the major-element composition of the SCLM.

DEFINITIONS

The "lithosphere" is generally regarded as the relatively rigid outer shell of the Earth, overlying a more ductile and mobile interior. McKenzie and Bickle (1988) formalised the concept of an outer mechanical boundary layer, in which heat transfer is by conduction, separated by a transition zone from an interior where heat transfer is by convection (and where the thermal gradient therefore is adiabatic). Considerable argument has followed, concerning the physical dimensions of the various boundary layers. Thermobarometric and isotopic studies on mantle-derived xenoliths with equilibrated granular microstructures suggest that the mechanical boundary layer may extend to at least 200–250 km beneath old cratonic areas (*e.g.*, Finnerty and Boyd, 1987), and has been maintained for periods in excess of 2–3 Ga (*e.g.*, Pearson *et al.*, 1995; Boyd *et al.*, 1997a). Such studies also imply that the mechanical boundary layer (beneath the continents, at least) is a chemical boundary layer as well, and is depleted relative to the underlying mantle. The issue has been complicated by some isotopic studies, which tend to equate different layers of Earth's structure with isotopically recognisable geochemical reservoirs (*e.g.*, Menzies, 1990), and by rheological arguments requiring a thin mechanical boundary layer that may be inconsistent with xenolith evidence [see a detailed critique by Anderson (1995)].

In this paper we use the term "lithospheric mantle" to refer to the uppermost portion of Earth's mantle, comprising both a mechanical and a chemical boundary layer, and characterised by conductive heat transfer. We suggest that the transition to an adiabatic geotherm occurs over a narrow interval, at least under the older parts of continents, and may be represented by a specific class of lithospheric xenoliths, the high-temperature sheared peridotites. We recognise that some xenoliths may be derived from below the lithosphere (as defined here) and that continental roots [the "tectosphere" of Jordan (1988)] may extend much deeper than the xenolith record.

To simplify the examination of temporal variation in lithosphere composition, we have modified Janse's (1994) classification of crustal regions, which is based on tectonothermal age (the last period of major thermal perturbation). In our terminology, *Archons* experienced their last major tectonothermal event more than 2.5 Ga ago, *Protons* between 2.5–1.0 Ga and *Tectons* less than 1.0 Ga (see Griffin *et al.*, 1998a).

This work considers only the composition of the ultrabasic component of the SCLM, assuming that the basic component is small (<1%?; Schulze, 1989), and recognising that it is extremely difficult to quantify. We further restrict the ultrabasic component to the Cr-diopside series of Wilshire and Shervais (1975), thus focussing on probable mantle wall-rocks and ignoring the younger magmatic component represented by their Al-augite series. While this dichotomy was first established with respect to spinel-facies xenoliths in alkali basalts, it can be extended to the garnet facies with little ambiguity (Harte, 1983; O'Reilly and Griffin, 1987). The term "harzburgite" will be used only for ultrabasic rocks without modal clinopyroxene, while those containing olivine + opx + cpx will be termed "lherzolites". While not in accord with standard petrographic schemes, this terminology emphasises the fundamental distinction between rocks saturated or undersaturated in Ca, and provides a distinction that can be recognised in garnet xenocrysts as well.

Some xenoliths rich in pyroxenes ± garnet represent modal variants of the Cr-diopside series; they should be counted into estimates of SCLM composition, but commonly are over-represented in the analysed suites, partly because of their attractive appearance. To avoid giving these an undue weight, we have arbitrarily rejected xenolith analyses with CaO or Al_2O_3 contents >6%. We have not excluded samples (with CaO or Al_2O_3 <6%) showing modal metasomatism (*e.g.*, by the presence of amphibole or mica), since these represent an important process affecting mantle composition.

SECULAR VARIATION IN SCLM COMPOSITION: PREVIOUS STUDIES

Boyd and coworkers (Boyd and Mertzman, 1987; Boyd, 1989, 1997a) have used the major-element compositions of mantle-derived xenoliths and oceanic peridotites to demonstrate a dichotomy between cratonic and circumcratonic mantle, with the implication of a marked difference in the processes that produced SCLM in Archean and Phanerozoic time. These differences are illustrated in a plot of olivine content (or olivine/opx ratio) against the Fo content of olivine (Fig. 1). In oceanic (or circumcratonic) peridotites, increasing depletion is accompanied by increasing olivine contents, and increasing whole-rock Mg/Si and mg# (or Fo content of olivine). In contrast, many xenoliths from Archean cratons, whether lherzolite or harzburgite, are characterised by low olivine/opx (low Mg/Si) despite the high degree of depletion shown by their high mg#, low Ca and Al, and low Ca/Al. This relationship is seen in xenoliths from both the Kaapvaal and Siberian cratons, which dominate the available database (Boyd *et al.*, 1997). Re-Os ages show that these cratonic xeno-

liths experienced their major depletion in Archean times (BOYD *et al.*, 1997; PEARSON *et al.*, 1995), while the circumcratonic mantle (and oceanic peridotites) apparently have undergone depletion during Proterozoic to Phanerozoic time (REISBERG and LORAND, 1995; LAMBERT *et al.*, 1995; MCBRIDE *et al.* 1996; HANDLER *et al.*, 1997)

A large proportion of the Cr-pyrope garnets included in diamonds have low-Ca, high-Cr compositions suggesting derivation from depleted harzburgitic parageneses, and garnet xenocrysts of these compositions are found almost exclusively in volcanic rocks that intrude Archons (Fig. 2A; GURNEY, 1984; GURNEY and ZWEISTRA, 1995; GRIFFIN and RYAN, 1995). This implies a fundamental difference in the SCLM between Archons and regions with younger crust. However, the garnet concentrates from SCLM of all ages are dominated by garnets of the lherzolite paragenesis, indicating that the overall composition of SCLM is lherzolitic. GRIFFIN *et al.* (1998a) showed that there is a continuous variation in the mean composition of these lherzolitic garnets, which correlates with the tectonothermal age of the crust intruded by their host volcanics (Fig. 2B), and that these data can be modelled in terms of a progressively less depleted SCLM composition through time. The correlation between SCLM composition and crustal age strongly suggests the quasi-simultaneous formation of mantle and crustal volumes,

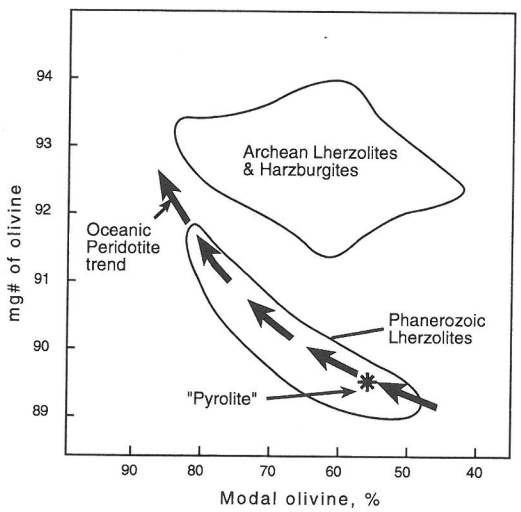

FIG. 1. Plot (after BOYD, 1989), illustrating the broad differences in olivine abundance and depletion index (mg# = 100 Mg/(Mg + Fe)) between oceanic peridotites and xenoliths of Archean mantle (Siberian and Kaapvaal cratons), and the similarity of most mantle xenoliths from Phanerozoic terrains to the oceanic trend, in these coordinates.

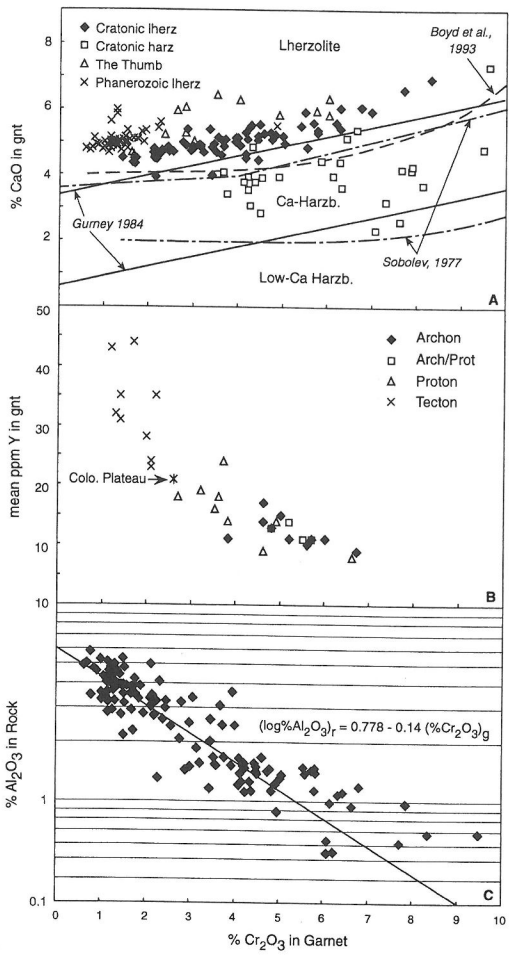

FIG. 2. Mantle-derived Cr-pyrope garnets. A. CaO-Cr_2O_3 plot (after GRIFFIN *et al.*, 1998a) showing garnet compositions from lherzolite and harzburgite xenoliths from mantle of different settings, and lines suggested by various authors to separate garnets from lherzolites, calcic harzburgites (cpx-free) and low-Ca harzburgites. We use the lines of GURNEY (1984) in this report. B. Mean Cr_2O_3 and Y contents of garnet concentrates from volcanic rocks, classed according to the tectonothermal age of the crust penetrated by the volcanic eruption. Archon/Proton designates areas with large volumes of Archean crust, but strongly reworked during Proterozoic time. After GRIFFIN *et al.* (1998a). C. Cr_2O_3 content of garnets from xenoliths, plotted against the Al_2O_3 content of the xenolith. The equation is for the line drawn through the data, which are from GRIFFIN *et al.* (1998a; Table 1).

and coupling between SCLM and crust over long time periods. If this is the case, it implies that lithospheric age may be the first-order control on SCLM composition, while tectonic setting is of lesser significance. This can be tested by examining the lithosphere beneath young crust in modern environments.

DATA SOURCES

Data on lithospheric mantle composition can be derived directly from three main sources: rock fragments (xenoliths) in volcanic rocks, crustal exposures (orogenic peridotite massifs, oceanic peridotites, ophiolite complexes) and xenocrysts of mantle minerals, especially garnet, in volcanic rocks. In the following we will outline characteristics of different xenolith suites and types of crustal peridotites, and compare these with mantle compositions calculated from suites of garnet xenocrysts. Table 1 gives median analyses (normalised to 100%) for a large number of sample suites (>1160 xenoliths, >380 crustal peridotites) divided by age and tectonic setting as explained below. References to primary data sources are given in Table 1.

Xenoliths

Xenoliths in volcanic rocks represent the most widespread and widely studied source of data on the SCLM. Their use is beset with problems: small size, heterogeneity, infiltration by the host magma, episodic metasomatism. In this work we attempt to circumvent these problems by inclusion of a large number of samples and by using median values (Table 1) rather than averages, to reduce distortion of compositions by small numbers of outliers.

Xenoliths from Tectons. The great majority of xenoliths for which analyses are available are from young volcanic rocks, especially intraplate basalts, in Tecton settings. In order to examine differences among modern tectonic settings, we have divided these into several groups (Table 1):
(1) YETI (Young extensional terrains, intraplate). Areas grouped in YETI (Table 1) show various combinations of active rifting, uplift and/or basin formation, high heat flow and sub-Moho mantle with anomalously low seismic velocities. These characteristics suggest that the basalts may be sampling recently created lithosphere.
(2) TILE (Tectons, incipient or little extension). Continental areas, which were not obviously extending at the time of eruption. Most of these areas are in western Europe, and many of the available Re-Os depletion ages are Proterozoic (COHEN *et al.*, 1996; MIESEL *et al.*, 1996b). The xenolith populations may be a mixture of older SCLM and the upwelling younger mantle that is visible in seismic tomography (HOERNLE *et al.*, 1995).
(3) OCEAN: Xenoliths in volcanic rocks on ocean islands. In many cases it is not clear what is being sampled – is it mid-ocean ridge (MOR) lithosphere, cumulates or new plume-related lithosphere? Kerguelen, which lies above a major oceanic plateau, is perhaps the most likely candidate for samples of plume-related lithosphere (MATTIELLI *et al.*, 1996). The Hawaiian xenoliths may represent cumulates from subcrustal magma chambers (SEN, 1987; CLAGUE, 1987).
(4) SUBD: Xenoliths in volcanic rocks from convergent-margin settings. Again, it is often difficult to know the origin of the samples: are they derived from subducted oceanic lithosphere, the mantle wedge above the slab, or upwelling mantle related to later back-arc rifting? The Itinome-gata xenoliths may represent the metasomatised mantle wedge (TANAKA and AOKI, 1979).

Xenoliths from Protons (PROT). There are few xenolith suites from areas with Proterozoic crust, and in some of these, such as the Colorado Plateau, younger uplift suggests recent modification of the SCLM may have occurred (PARSONS and MCCARTHY, 1995; RITER and SMITH, 1996). In our data set, the samples from Obnazhennaya (N. Siberia), Louwrencia (Namibia), and Mt. Gambier (South Australia) are least ambiguous. The Obnazhennaya and Louwrencia kimberlites are intruded through unmodified Proterozoic crust, and the xenoliths from Namibia have Re-Os depletion ages of 1.8–2.2 Ga (GRIFFIN *et al.*, 1998d; HOAL *et al.*, 1995). The Tertiary basalts of Mt. Gambier penetrate a Proterozoic craton that experienced a late Proterozoic folding, and spinel peridotite xenoliths from Mt. Gambier have yielded a Re-Os isochron age of 1.9 Ga (HANDLER *et al.*, 1997). The Argyle xenolith data (JAQUES *et al.*, 1990) are reconstituted from highly altered material; the Argyle lamproite intrudes a Proterozoic mobile belt, and only lherzolitic garnets have been recovered from it, but rare inclusions of subcalcic pyrope in Argyle diamonds suggest that the mantle may contain some harzburgites, which are typical of Archean, rather than Proterozoic, mantle (JAQUES *et al.*, 1989; O'REILLY *et al.*, 1997).

Xenoliths from Archons (ARK). The Archon database is dominated by xenoliths from the Kaapvaal craton of southern Africa. GRIFFIN *et al.* (1995) documented a major change in lithosphere thickness and composition beneath the Kaapvaal craton that took place ≈90 Ma ago. Most xenoliths described in the literature are derived from kimberlites intruded after this time, and they therefore may be a biased sample. The only other large set of xenoliths is from the Siberian craton, and nearly all data are from the Udachnaya kimberlite pipe (BOYD *et al.* 1997; UKHANOV *et al.*, 1988). The xenolith analyses from the Slave craton of Canada have been constructed from modal analysis of small (1–2 cm) samples (PEARSON *et al.*, 1998; authors' unpubl. data), and may be biased toward olivine-rich compositions (Table 1). We have separated the ARK xenoliths into two microstructural groups – granular and sheared – and only the former are plotted in the figures, while the latter are discussed separately.

Orogenic Massifs

This group (MAS) includes a large number of peridotite bodies that are distinguished from ophiolitic peridotites by a lack of any obvious association with other rocks of oceanic provenance. Many also are associated with granulites of apparent mid- to lower-crust origin (FOUNTAIN and SALISBURY, 1981). These massifs are widely interpreted as slices of SCLM (MENZIES and DUPUY, 1991), although there is dispute about some, such as Lanzo, which is variously interpreted as oceanic or continental (*e.g.*, NICOLAS *et al.*, 1980). Some of these bodies (especially Caussou) are heavily metasomatised, as shown by abundant amphibole and mica, and by anomalous Ca/Al ratios (FABRIES *et al.*, 1989). Re-Os depletion ages of 1.5–2.2 Ga on several Pyreneean and Swiss massifs and Ronda (REISBERG and LORAND, 1995; MEISEL *et al.*, 1996a) suggest that at least these bodies represent Proterozoic SCLM, possibly modified during Mesozoic emplacement into the crust. The Norwegian garnet peridotite massifs represent subcontinental mantle emplaced into Proterozoic crust during the Caledonian orogeny. Some have yielded Proterozoic Sm-Nd mineral ages (JAMTVEIT *et al.*, 1991), and may be relatively unmodified Proton SCLM; they therefore have been included in the PROT dataset.

Oceanic Peridotites (Abyssal peridotites, Ophiolites)

There are many analyses of abyssal oceanic peridotites (AOP), but nearly all of these rocks have undergone heavy

Table 1. Median compositions of sample suites

Group	YETI (Young Extensional Tectons, Intraplate)							
Locality	Australia NSW, VIC, QLD	Hungary	Romania	W. N America	Siberia/ Mongolia	Siberia/ Mongolia	E. China	E. China
rock type	sp per.	sp per.	sp per.	sp per.	sp per.	gt lherz.	sp per.	gt lherz.
No. Analyses	253	20	22	75	32	16	117	17
References*	1-9	10	11	14-20	21-25	23,24	26-31	28,31
SiO_2	44.55	43.79	44.23	44.37	44.40	44.54	44.95	45.48
TiO_2	0.08	0.09	0.11	0.11	0.10	0.16	0.10	0.16
Al_2O_3	2.46	2.35	2.96	3.12	3.13	3.95	2.92	3.80
Cr_2O_3	0.40	0.42	0.39	0.38	0.40	0.37	0.42	0.44
FeO_t	8.64	8.17	8.15	8.12	7.94	8.00	8.10	8.16
MnO	0.14	0.12	0.13	0.13	0.13	0.00	0.13	0.14
MgO	40.76	42.65	40.80	39.96	40.13	39.29	40.15	38.05
CaO	2.43	2.21	2.70	2.93	2.71	3.19	2.47	3.27
Na_2O	0.23	0.18	0.16	0.22	0.20	0.32	0.23	0.23
K_2O	0.03	0.01	0.01	0.01	0.02	0.03	0.04	0.03
P_2O_5	0.06	0.02	0.01	0.01	0.00	0.00	0.00	0.00
NiO	0.26	0.30	0.29	0.25	0.27	0.25	0.25	0.24
atomic ratios								
mg#	89.1	90.3	89.9	89.8	90.0	89.8	89.8	89.3
Mg/Si	1.35	1.46	1.38	1.35	1.35	1.32	1.34	1.25
Ca/Al	0.87	0.86	0.83	0.86	0.79	0.74	0.77	0.79
Cr/Cr+Al	0.10	0.11	0.08	0.08	0.08	0.06	0.09	0.07
Fe/Al	2.49	2.46	1.95	1.85	1.80	1.43	1.97	1.52
av. % ol	69	71	66	65	63	54	59	61
%Fo in ol	88.8	90.4	89.5	89.6	90.0	89.8	90.2	89.0

* 1, BURWELL (1975); 2, CHEN *et al.* (1989); 3, FREY and GREEN (1974); 4, FREY *et al.* (1989); 5, MCCARRON (1997); 6, O'REILLY and GRIFFIN (1987, 1998); 7, STOLZ and DAVIES (1988); 8, WILKINSON (1969, 1975); 9, WILSHIRE and BINNS (1961); 10, DOWNES *et al.* (1992); 11, VASELLI *et al.* (1995a); 12, HEINRICH and BESCH (1992); 13 WILSHIRE and SHERVAIS (1975); 14, LIANG and ELTHON (1990); 15, NIMZ *et al.* (1995); 16, FREY and PRINZ (1978); 17, *Bas. Volc. Study Proj.* (1981); 18, STOSCH (1980); 19, RODEN *et al.* (1988); 20, FEIGENSON (1986); 21, IONOV *et al.* (1992, 1993); 22, IONOV and HOFFMAN (1995); 23, WIECHERT *et al.* (1995); 24, PRESS *et al.* (1986); 25, STOSCH *et al.* (1986); 26, LIU and FAN (1990); 27, QI *et al.* (1995); 28, SONG and FREY (1989); 30, CAO and ZHU (1987); 31, XU *et al.* (1998); 32, STOSCH and SECK (1980); 33, PAUL (1971); 34, STOSCH and LUGMAIR (1986); 35, HARTMAN and WEDEPOHL (1990); 36, VASSELLI *et al.* (1995b); 37, LORAND and ALARD (1998); 39, ALARD *et al.* (1996); 41, BERGER (1964, 1981); 42, BROUSE (1961, 1968); 43, CAUSSE (1965); 44, DOWNES and DUPUY (1987); 45, HUTCHINSON *et al.* (1986); 46, LENOIR *et al.* (1997); 47, CHIARAMONTI *et al.* (1986); 48, DAUTRIA and GIROD (1986); 49, DUPUY *et al.*, 1986); 50, BODINIER (1988); 51, FREY *et al.* (1985); 52, CONQUERE (1970); 53, BOUDINIER *et al.* (1988); 54, ERNST (1978); 55, ERNST and PICARDO (1979); 56, BECKER (1996); 57, OTTENELLO *et al.* (1984); 58, BONATTI *et al.* (1981, 1986); 59, BONATTI and MICHAEL (1989); 60, DUPUY *et al.* (1987); 61, AOKI and SHIBA (1973); 62, MCDONOUGH (unpub.); 63, MAURY *et al.* (1992); 64, JAQUES *et al.* (1983); 65, JAQUES and CHAPPELL (1980); 66, LONEY *et al.* (1971); 67, LIPPARD *et al.* (1986); 68, KUNO and AOKI (1970); 69, SEN and LEEMAN (1991); 70, SEN (1988); 71, QI *et al.* (1994); 72, GREGOIRE (unpubl.); 73, SIENA *et al.* (1991); 74, MICHAEL and BONATTI (1985); 75, AUMENTO and LOUBERT (1971); 76, NIU and HEKINIAN (1997); 77, HEBERT *et al.* (1983); 78, NIU (pers. comm.); 79, D. SMITH (pers. comm.); 80, EHRENBERG (1979); 81, SMITH and LEVY (1976); 82, SMITH (1979); 83, AOKI (1981); 84, SMITH and RITER (1997); 85, LAUGHLIN *et al.* (1971); 86, KUDO *et al.* (1972); 87, SPETSIUS and SERENCO (1990); 88, F. R. BOYD (pers. comm.); 89, JAQUES *et al.* (1990); 90, CARSWELL (1968); 91, ROST (unpubl.); 92, BOYD *et al.* (1997); 93, CARSWELL *et al.* (1984); 94, GRIFFIN *et al.* (unpubl.); 95, CARSWELL *et al.* (1979); 96, BOYD and MERTZMAN (1987); 97, WALKER *et al.* (1989); 98, CARSWELL and DAWSON (1970); 99, COX *et al.* (1973); 100, DANCHIN (1979); 101, NIXON and BOYD (1973); 102, COX *et al.* (1987); 103, BOYD *et al.* (1993); 104, NIXON (1987).

Table 1. (Cont.)

Group	TILE (Tectons, Incipient or Little Extension)					
Locality	Germany Dreis. Weiher	Germany Eifel	Germany Hessian Depr.	France Massif Cent.	Brazil/ Paraguay	Algeria
rock type	sp per.	sp per.	sp per.	sp per.	sp per.	sp per.
No. Analyses	15	16	48	72	10	24
References*	32,33	34	35,36	37-46	47	48,49
SiO_2	43.87	43.20	44.07	44.08	43.67	44.97
TiO_2	0.19	0.02	0.04	0.10	0.05	0.11
Al_2O_3	1.50	1.39	1.61	2.10	1.61	2.33
Cr_2O_3	0.36	0.42	0.40	0.39	0.40	0.37
FeO_t	8.69	7.61	8.26	8.08	8.38	8.32
MnO	0.13	0.14	0.13	0.12	0.14	0.14
MgO	42.53	43.74	43.02	41.81	43.18	40.18
CaO	1.80	1.16	1.72	2.19	1.15	2.52
Na_2O	0.18	0.11	0.12	0.11	0.20	0.18
K_2O	0.02	0.05	0.05	0.03	0.39	0.01
P_2O_5	0.00	0.00	0.01	0.00	0.02	0.05
NiO	0.00	0.29	0.29	0.27	0.30	0.26
atomic ratios						
mg#	89.7	91.1	90.3	90.2	90.2	89.6
Mg/Si	1.45	1.51	1.46	1.42	1.48	1.33
Ca/Al	1.09	0.76	0.98	0.95	0.73	0.89
Cr/Cr+Al	0.14	0.17	0.14	0.11	0.14	0.10
Fe/Al	4.10	3.88	3.63	2.73	3.68	2.54
av. % ol			71	70		
%Fo in ol			89.9	89.7		

Table 1. (Cont.)

Group	MASS (Orogenic Massifs)								
Locality	Lanzo	Ronda	Caussou	Balmuccia	Pyrenees	Lherz	Austria	Internal Ligurides	Zarbagad
rock type	sp per.	sp per.	sp per.	sp per.	sp per.	sp per.	sp per.	sp per.	sp per.
No. Analyses	22	16	14	7	24	24	25	20	23
References*	50	51	50,52,53	54,55	53,55	53,55	56	55,57	58,59
SiO_2	45.65	44.36	45.21	47.34	45.24	44.53	45.45	45.02	44.45
TiO_2	0.10	0.08	0.21	0.13	0.12	0.13	0.06	0.18	0.11
Al_2O_3	2.58	2.64	3.38	1.46	2.88	1.56	1.99	3.28	3.91
Cr_2O_3	0.37	0.37	0.30	0.39	0.34		0.43	0.35	0.38
FeO_t	8.07	8.08	8.08	7.45	8.02	8.26	7.92	8.02	8.50
MnO	0.13	0.13	0.13	0.12	0.12	0.00	0.13	0.13	0.14
MgO	39.91	41.18	38.58	40.11	39.82	42.53	42.16	40.48	39.33
CaO	2.60	2.55	3.92	2.71	2.79	1.18	1.38	1.80	3.06
Na_2O	0.27	0.28	0.00	0.24	0.00	0.00	0.06	0.24	0.35
K_2O	0.09	0.20	0.43	0.00	0.24	0.14	0.01	0.15	0.02
P_2O_5	0.03	0.01	0.07	0.00	0.00	0.00	0.02	0.01	0.00
NiO	0.27	0.28		0.24	0.26		0.32	0.25	0.26
atomic ratios									
mg#	89.8	90.1	89.5	90.6	89.9	90.2	90.5	90.0	89.2
Mg/Si	1.31	1.39	1.27	1.27	1.31	1.43	1.39	1.34	1.32
Ca/Al	0.92	0.88	1.06	1.69	0.89	0.69	0.63	0.50	0.71
Cr/Cr+Al	0.09	0.09	0.06	0.15	0.07		0.13	0.07	0.06
Fe/Al	2.22	2.17	1.69	3.62	1.98	3.75	2.82	1.73	1.54
av. % ol		73		65	60		58		50
%Fo in ol		90.5		90.0	90.0		89.0		89.0

Table 1. (Cont.)

Group	SUBD (Convergent margin xen.)			OPH (Conv. margin		Ophiolites)	High-T Sheared Lherz.	
Locality	Italy Sardinia	Japan Itinome-gata	Phillipines Bataan	PNG	USA Burro Mtn.	Oman Semail	Russia Udachnaya	S. Africa Kaapvaal
rock type	sp per.	sp per.	sp per.	sp per.	sp per.	sp per.	gt per.	gt per.
No. Analyses	12	15	7	7	8	16	18	48
References*	60	61,62	63	64,65	66	67	92	96,100-3
SiO_2	44.15	44.77	45.32	43.60	43.92	44.55	44.24	44.30
TiO_2	0.04	0.13	0.03	0.00	0.01	0.03	0.11	0.17
Al_2O_3	1.31	2.73	1.23	0.06	0.95	1.42	0.80	1.74
Cr_2O_3	0.36	0.38	0.31	0.38	0.43	0.40	0.42	0.30
FeO_t	7.94	8.40	7.81	7.01	7.80	8.28	7.99	8.14
MnO	0.13	0.13	0.14	0.12	0.12	0.14	0.13	0.12
MgO	44.63	40.02	43.85	48.42	46.02	42.50	44.32	43.28
CaO	1.30	2.78	0.87	0.04	0.65	1.22	1.11	1.27
Na_2O	0.10	0.16	0.06	0.01	0.01	0.00	0.10	0.12
K_2O	0.01	0.03	0.02	0.00	0.00	0.00	0.08	0.05
P_2O_5	0.03	0.00	0.01	0.00	0.00	0.00	0.00	0.00
NiO	0.30	0.26	0.31	0.33	0.32	0.31	0.29	0.26
atomic ratios								
mg#	90.9	89.5	90.9	92.5	91.3	90.2	90.8	90.5
Mg/Si	1.51	1.34	1.45	1.66	1.57	1.43	1.50	1.46
Ca/Al	0.90	0.93	0.64	0.67	0.63	0.78	1.26	0.67
Cr/Cr+Al	0.16	0.09	0.15	0.82	0.24	0.16	0.26	0.10
Fe/Al	4.29	2.18	4.49	89.30	5.84	4.13	7.04	3.32
av. % ol							71	69
%Fo in ol							91.2	91.2

Table 1. (Cont.)

Group	OCEAN (Ocean Islands)				AOP (Abyssal Peridotites)			
Locality	Hawaii	Tahiti	Kerguelen	Lanzarote	FAMOUS	MAR	EPR	Calc. from modes (Niu)
rock type	sp per.	sp per.	sp per.	sp per.	sp per.	sp per.	sp per.	sp per.
No. Analyses	14	10	26	22	7	8	12	120
References*	68-70	71	72	73	74	75	76,77	78
SiO_2	44.43	43.87	43.80	43.05	45.74	44.37	44.96	43.61
TiO_2	0.13	0.04	0.04	0.02	0.02	0.08	0.06	0.02
Al_2O_3	2.29	1.64	0.82	0.84	0.92	2.61	0.78	1.62
Cr_2O_3	0.32	0.40	0.45	0.44	na	0.39	0.36	0.66
FeO_t	8.38	8.57	8.37	7.64	7.67	8.45	10.25	8.51
MnO	0.13	0.15	0.14	0.12	0.12	0.17	0.14	0.00
MgO	41.30	42.53	45.50	46.65	44.47	42.87	42.45	43.96
CaO	1.93	1.42	0.69	0.72	0.37	0.31	0.86	1.38
Na_2O	0.28	0.02	0.00	0.11	0.14	0.28	0.00	0.04
K_2O	0.00	0.01	0.00	0.02	na	na	na	na
P_2O_5	0.07	0.00	0.02	0.01	na	na	na	na
NiO	0.00	0.00	0.30	0.31	na	0.25	0.27	na
atomic ratios								
mg#	89.8	89.8	90.7	91.5	91.2	90.1	88.1	90.2
Mg/Si	1.39	1.45	1.55	1.62	1.45	1.44	1.41	1.51
Ca/Al	0.77	0.79	0.77	0.81	0.37	0.11	1.01	0.84
Cr/Cr+Al	0.09	0.14	0.27	0.26	-	0.09	0.24	0.21
Fe/Al	2.60	3.71	7.24	6.42	5.91	2.30	9.32	3.72
av. % ol		62	81	81				74
%Fo in ol		89.5	89.8	91.4				90.0

Table 1. (Cont.)

Group	PROT (Prot. Cratons)					
Locality	USA Colorado Plat.	Russia Obnazhennaya	Australia Mt. Gambier	Namibia Louwrencia	Australia Argyle	Norway Massifs
rock type	sp gt per.	sp gt per.	sp per.	gt per.	gt per.	sp gt per.
No. Analyses	30	19	19	24	4	32
References*	79-86	87	5	88	89	90,91
SiO_2	44.20	42.58	44.22	44.67	45.47	43.72
TiO_2	0.09	0.00	0.04	0.03	0.05	0.01
Al_2O_3	1.70	1.77	1.83	0.93	0.90	1.13
Cr_2O_3	0.41	0.42	0.44	0.34	0.27	0.38
FeO_t	7.91	8.43	7.61	7.65	6.64	7.16
MnO	0.12	0.13	0.13	0.12	0.07	0.12
MgO	42.75	44.66	43.45	44.58	45.37	45.84
CaO	1.37	1.36	1.56	0.84	0.67	0.39
Na_2O	0.17	0.06	0.05	0.04	0.02	0.07
K_2O	0.02	0.00	0.00	0.01	0.26	0.02
P_2O_5	0.00	0.00	0.00	0.02	0.02	0.00
NiO	0.00	0.26	0.29	0.31	0.32	0.33
atomic ratios						
mg#	90.4	90.4	91.2	91.1	92.4	91.8
Mg/Si	1.44	1.57	1.47	1.48	1.49	1.55
Ca/Al	0.79	0.70	0.73	0.72	0.69	0.35
Cr/Cr+Al	0.14	0.14	0.14	0.20	0.17	0.19
Fe/Al	3.31	3.38	2.95	5.83	5.24	4.49
av. % ol			72		77	
%Fo in ol			91.0		92.3	

Table 1. (Cont.)

Group	ARK (Archean Peridotite Xenoliths)						
Locality	Russia Udachnaya	Russia Udachnaya	Russia Udachnaya	S. Africa Kaapvaal	S. Africa Kaapvaal	S. Africa Kaapvaal	Canada A154, Slave
rock type	sp per.	gt harz.	gt lherz.	gt lherz.	gt harz.	sp per.	gt per.
No. Analyses	9	3	18	79	24	17	14
References*	92	92	92	93-102	100-104	93	94
SiO_2	44.69	42.17	44.29	46.39	45.92	45.07	42.9
TiO_2	0.02	0.09	0.04	0.06	0.05	0.05	0.0
Al_2O_3	1.07	0.61	1.04	1.42	1.18	0.71	1.1
Cr_2O_3	0.31	0.37	0.37	0.35	0.29	0.37	0.5
FeO_t	6.65	7.45	7.58	6.56	6.44	6.43	7.2
MnO	0.11	0.10	0.13	0.11	0.09	0.11	0.1
MgO	45.43	47.80	45.17	43.35	45.25	45.59	47.2
CaO	0.55	1.02	0.96	0.95	0.54	0.52	0.6
Na_2O	0.05	0.07	0.07	0.10	0.09	0.10	0.0
K_2O	0.15	0.10	0.10	0.08	0.05	0.10	0.0
P_2O_5	0.01	0.01	0.02	0.03	0.04	0.03	0.0
NiO	0.31	0.31	0.29	0.28	0.27	0.32	0.3
atomic ratios							
mg#	92.4	92.0	91.4	92.2	92.6	92.7	92.1
Mg/Si	1.52	1.69	1.52	1.40	1.47	1.54	1.64
Ca/Al	0.47	1.53	0.84	0.61	0.42	0.64	0.50
Cr/Cr+Al	0.16	0.29	0.19	0.14	0.14	0.26	0.23
Fe/Al	4.40	8.70	5.16	3.28	3.87	6.41	4.71
av. % ol	69	83	69	61	65	69	79
%Fo in ol	92.8	92.6	92.4	92.3	93.5	92.8	91.7

serpentinisation, and their compositions (especially Ca and Fe contents and Ca/Al ratios) have been strongly modified (Table 1). NIU (1997; pers. comm.) has attempted to circumvent this problem by combining EMP analysis of relict primary minerals with detailed modal analysis of samples where primary mineralogy is still recognisable in the microstructures, to calculate the original rock composition. This data set will be used here, with reservations as stated below. Ophiolites (OPH) commonly offer fresher samples, but it is often not clear in the literature whether deformed cumulate peridotites have been clearly distinguished from tectonite peridotites. In some cases there also is disagreement about the original tectonic setting (convergent margin or MOR) of individual bodies. The Internal Ligurides may represent a MOR ophiolite fragment (ERNST, 1978; ERNST and PICCARDO, 1979). The median compositions shown in Table 1 for convergent-margin ophiolites cover most of the range of depletion observed in this group.

Zabargad

The peridotites on Zabargad Island in the Red Sea have been uplifted and exposed by Cenozoic rifting of continental crust, and are compositionally distinct from abyssal peridotites or ophiolites; they apparently represent very fertile subcontinental lithosphere. Spinel-, plagioclase-, and amphibole peridotites occur on Zabargad, but there are no significant major-element compositional differences among these (BONATTI *et al.*, 1986). Very similar material occurs as xenoliths in alkali basalts in nearby Saudi Arabia (MCGUIRE, 1988a,b).

Cr-pyrope garnet xenocrysts – calculation of SCLM composition

Cr-pyrope is a minor but widespread phase in the SCLM, and garnet grains routinely are recovered in the course of diamond exploration programs (GURNEY and ZWEISTRA, 1995; GRIFFIN and RYAN, 1995). They will be used in this work to provide estimates of mean composition of mantle volumes. The Cr content of garnet in ultramafic rocks is well-correlated with the Al content of the host rocks (Fig. 2C). The contents of other major elements in such ultramafic rocks are, in turn, well-correlated with Al_2O_3 (Fig. 3). We have used these correlations to derive an internally consistent set of equations (Table 2) that can be used to calculate the composition of an ultramafic rock suite, given the median Cr content of its garnets. The scatter of points in Fig. 2C and Fig. 3 ensures that this procedure will only yield reasonable results for a statistically significant data set. We will use the Ca-Cr relationships of garnets (Fig. 2A) from xenoliths to divide garnets into harzburgitic and lherzolitic parageneses, and will calculate mean rock compositions for each type separately.

Table 3 shows median compositions ("Gnt-SCLM") of lherzolite and harzburgite from the Kaapvaal craton (calculated from garnets in kimberlites <90 Ma old); these are compared with median compositions of lherzolitic and harzburgitic xenoliths from the same group of kimberlites. The agreement for all major, and many minor, elements is excellent. Similar agreement is obtained between Gnt-SCLM (based on garnet xenocrysts in alkali basalts) and garnet peridotite xenoliths from the Tectons of eastern China and the Vitim area, Siberia. The Gnt-SCLM calculated using concentrates from the Obnazhennaya kimberlite of northern Siberia is less depleted (higher Al, Ca) than the median lherzolite xenolith from this pipe. However, Obnazhennaya contains many (cpx + gnt)-rich xenoliths of the Cr-diopside series (SPETSIUS, 1995), which were excluded from the calculated xenolith median by the 6%-Al_2O_3 screen mentioned above. In this case, the Gnt-SCLM may give the better picture of the mean composition of the SCLM.

The median composition of spinel peridotite xenoliths from Mt Gambier (South Australia) is very similar to the Gnt-SCLM calculated using concentrates from several South Australian kimberlites, located ca 300 km west of Mt. Gambier in the same Proterozoic craton. Calculated lherzolite and harzburgite compositions from the Daldyn kimberlite field of Siberia are lower in Fe and Ca than the median analyses of the xenoliths from Udachnaya. This difference reflects the late-stage metasomatic introduction of Fe and Ca into these xenoliths, described by BOYD *et al.* (1997); in this case the compositions calculated from the garnets are closer to the compositions estimated by modal analysis/EMP reconstruction of the xenoliths (BOYD *et al.*, 1997).

To calculate the mean composition of individual mantle sections from garnet data, we have first used temperature estimates based on Nickel Thermometry (GRIFFIN *et al.*, 1989b; RYAN *et al.*, 1996) to place the grains from each locality in stratigraphic order. Garnets with T_{Ni} >1100°C commonly also show high Ti, Zr and Y contents, reflecting the effects of high-T melt metasomatism (GRIFFIN and RYAN, 1995; GRIFFIN *et al.*, 1998c), and these have been excluded from the calculation. We then have used the Ca-Cr relationships (Fig. 2A) to estimate the relative proportions of harzburgite and lherzolite, and the median Cr contents in garnets of each type in the temperature interval 600–1100°C have been used to calculate rock compositions. These were then combined in a weighted mean to give the composition of the SCLM (Table 4). This procedure allows us to use a database of diamond-exploration samples (≈6000 analyses used here) to examine a wider spectrum of mantle sections than would be possi-

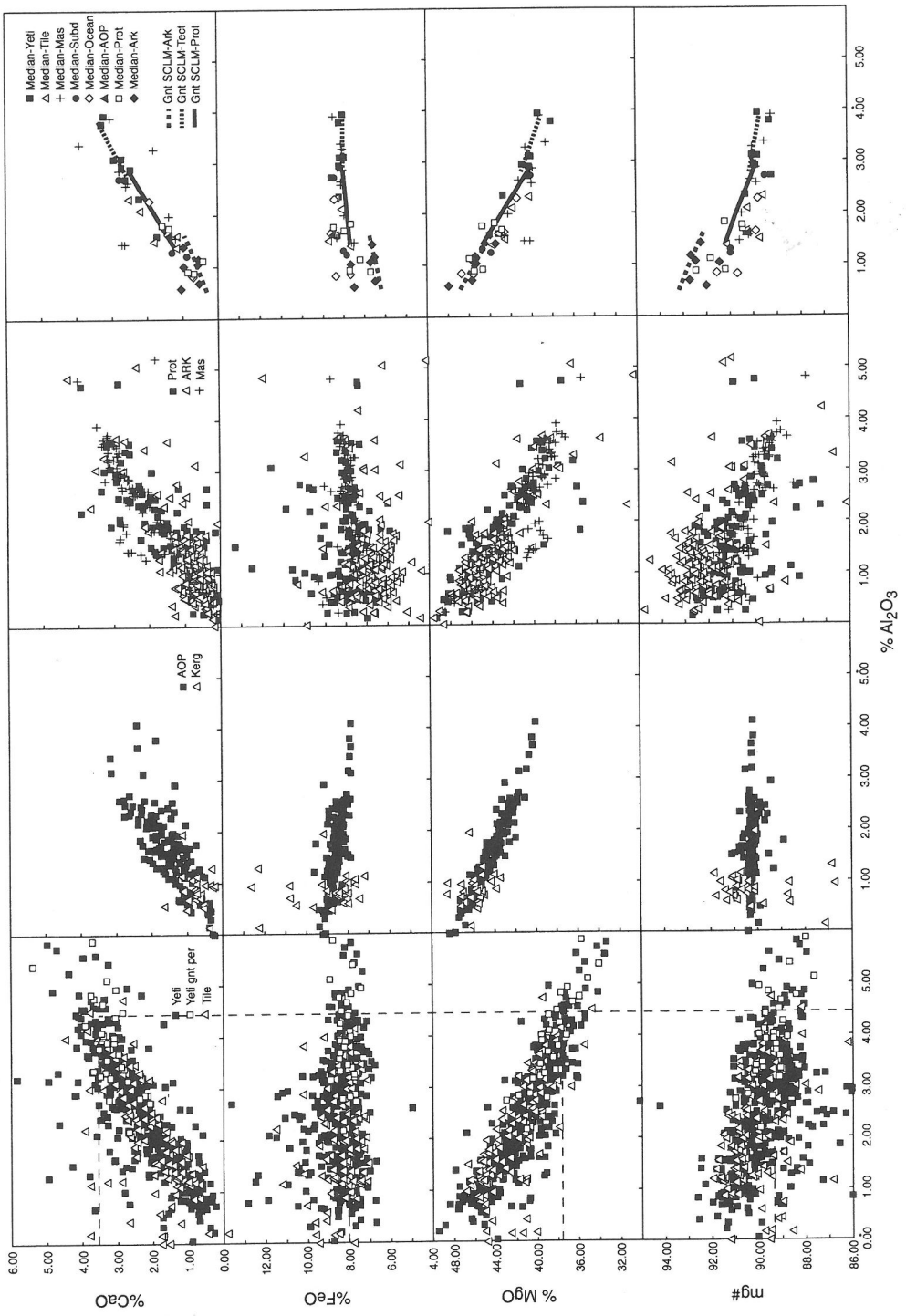
Median-Yeti
Median-Tile
Median-Mas
Median-Subd
Median-Ocean
Median-AOP
Median-Prot
Median-Ark
Grt SCLM-Ark
Grt SCLM-Tect
Grt SCLM-Prot
Yeti
Yeti grt per Tile
AOP
Kerg
Prot
ARK
Mas
%CaO
%FeO
% MgO
mg#
% Al_2O_3

FIG 3A

FIG 3B

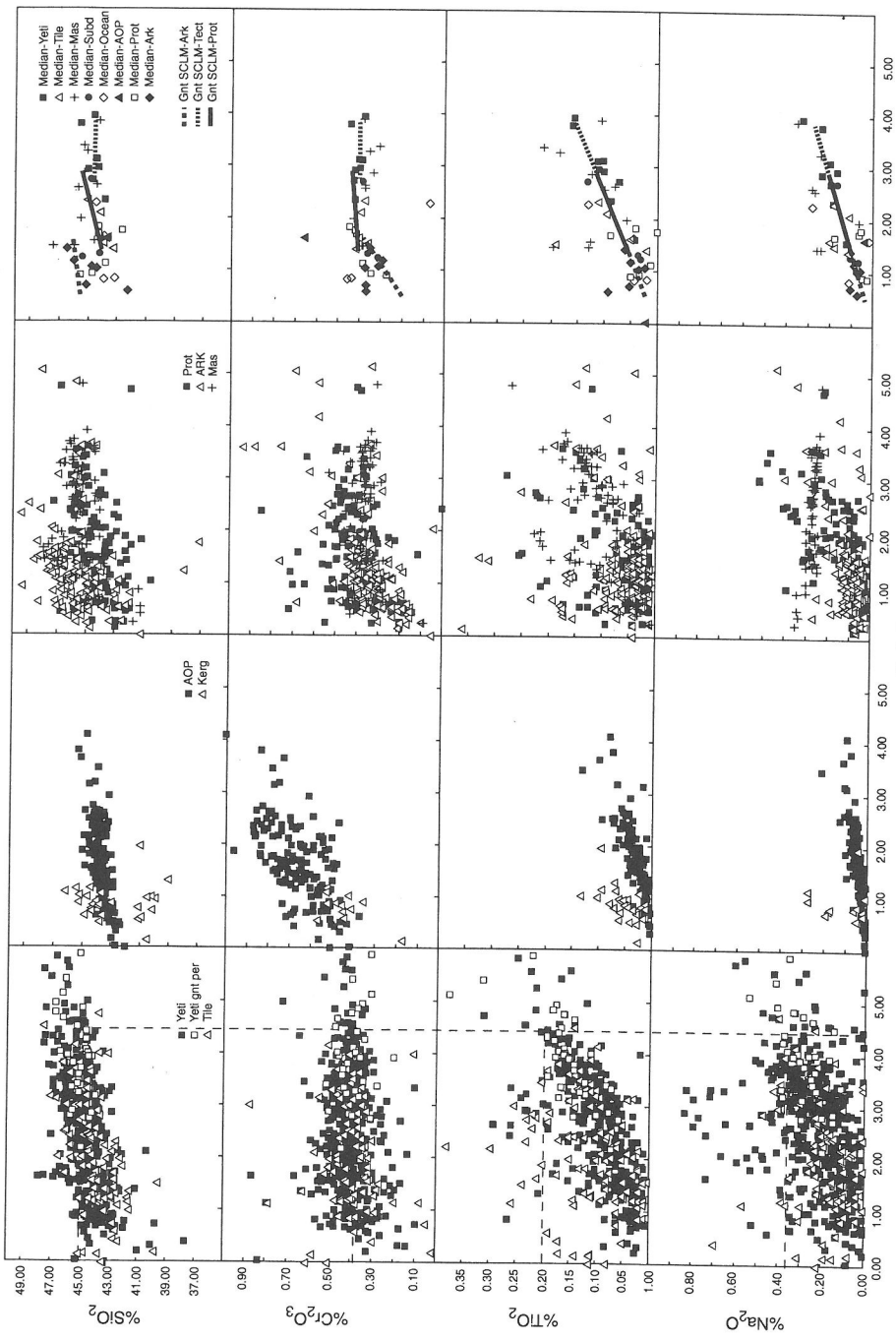

FIG. 3. Concentrations of major and minor elements in xenoliths and crustal peridotites, plotted against Al_2O_3 content; suites listed in Table 1. Right-hand panel of each row shows median values (Table 1) and ranges of SCLM composition calculated from garnet concentrates (Table 4). Horizontal and vertical dashed lines in left-hand panel show the Primitive Upper Mantle compositions of McDONOUGH and SUN (1990). mg# = 100Mg/(Mg + Fe) (atomic ratio). *Data sets* (Table 1): AOP, abyssal peridotites; ARK, Archon xenoliths; Kerg, Kerguelen Is.; Prot, Proton xenoliths and massifs; Mas, W. European massifs; Tile, Tectons, little extension; Yeti, young extensional Tectons.

Table 2. Regressions used in calculating SCLM from Garnets

1. log $\%Al_2O_3$ in rock = 0.778-0.14($\%Cr_2O_3$ in gnt)

Archons:
2. $\%MgO = 48.3-3(\%Al_2O_3)$
3. $\%FeO = 5.9 +0.5(\%Al_2O_3)$
4. $\%Cr_2O_3 = 0.12 + 0.16(\%Al_2O_3)$
5. $\%CaO = 0.6(\%Al_2O_3)$
6. $\%MnO = 0.07 + 0.017(\%FeO-4)$
7. $\%TiO_2 = 0.04(\%Al_2O_3)$
8. $\%Na_2O = 0.07(\%Al_2O_3)$

Tectons: As for Archons, except
9. $\%MgO = 46-1.9(\%Al_2O_3)$ where $\%Al_2O_3 \geq 1.5$
10. %FeO = 8
11. $\%Cr_2O_3 = 0.4$
12. <2.5% CaO: $\%CaO = 0.88(\%Al_2O_3)$
    >2.5% CaO: $\%CaO = 0.5 + 0.7(\%Al_2O_3)$
13. %MnO = 0.13

Protons: As for Tectons, except
14. $\%MgO = 49-3.1(\%Al_2O_3)$
15. $\%FeO = 7.4 +0.21(\%Al_2O_3)$
16. $\%Cr_2O_3 = 0.375 + 0.02(\%Al_2O_3)$

ble from the limited xenolith data, especially in Archons and Protons.

COMPOSITIONAL DATA

Major oxides vs Al_2O_3

Figure 3 shows several oxides plotted against Al_2O_3, which is a convenient measure of depletion in basaltic components (FREY and GREEN, 1974; NORMAN, 1998), for several of the data groupings shown in Table 1 and discussed above. The first three panels in each row show the scatter of data for individual groups; the final panel shows the median values for individual localities or subsets within each group (from Table 1), and the range of Gnt-SCLM (Table 4) for each tectonic setting. Vertical and horizontal lines in the first panel of each row mark the Primitive Mantle values of MCDONOUGH and SUN (1995) for reference.

CaO. The data from YETI, TILE, MAS and PROT show a well-defined positive correlation, with a

Table 3. Comparisons of garnet-SCLM with median analyses of xenolith suites

	Kaapvaal<90Ma Calc. Gt Lherz	Kaapvaal Median Lherz Xen	Kaapvaal<90Ma Calc. Gt Harz	Kaapvaal Median Harz Xen	Daldyn Calc. Gt Lherz	Daldyn Median Lherz Xen.	Daldyn Calc. Gt Harz	Daldyn Median Harz. Xen.
no. samples	335	79	64	24	390	18	180	3
SiO_2	46.0	46.6	45.7	45.9	45.8	44.3	45.4	42.2
TiO_2	0.07	0.06	0.04	0.05	0.05	0.04	0.02	0.09
Al_2O_3	1.7	1.4	0.9	1.2	1.2	1.0	0.4	0.6
Cr_2O_3	0.40	0.35	0.26	0.27	0.31	0.37	0.18	0.37
FeO	6.8	6.6	6.3	6.4	6.5	7.6	6.1	7.4
MnO	0.12	0.11	0.11	0.09	0.11	0.13	0.11	0.10
MgO	43.5	43.5	45.8	45.2	44.9	45.2	47.2	47.8
CaO	1.0	1.0	0.5	0.5	0.7	1.0	0.2	1.0
Na_2O	0.12	0.10	0.06	0.09	0.08	0.07	0.03	0.07
NiO	0.27	0.28	0.30	0.27	0.29	0.29	0.32	0.31

	S. Australia Calc. Gt Lherz.	Mt. Gambier(SA) Median Xen.	Obnazhennaya Calc. Gt Lherz.	Obnazhennaya Med. Lherz. Xen.	E. China Calc. Gt Lherz	E. China Med. Lherz. Xen.	Vitim Calc. Gt Lherz.	Vitim Med. Lherz. Xen.
no. samples	365	19	160	19	150	17	30	16
SiO_2	44.4	44.2	44.9	42.6	44.5	45.5	44.5	44.5
TiO_2	0.07	0.04	0.09	0.00	0.15	0.16	0.15	0.16
Al_2O_3	1.9	1.9	2.4	1.8	3.8	3.8	3.7	4.0
Cr_2O_3	0.41	0.44	0.42	0.44	0.40	0.44	0.40	0.37
FeO	7.8	7.6	7.9	8.4	8.0	8.2	8.0	8.0
MnO	0.13	0.13	0.13	0.13	0.13	0.14	0.13	na
MgO	43.2	43.5	41.7	44.7	39.1	38.1	39.3	39.3
CaO	1.6	1.6	2.1	1.4	3.4	3.3	3.3	3.2
Na_2O	0.13	0.05	0.17	0.06	0.27	0.23	0.26	0.32
NiO	0.30	0.29	0.28	0.26	0.25	0.25	0.25	0.25

Notes: Lherzolite and harzburgite garnets classified according to Figure 2A. Al_2O_3 for rock type corresponding to each garnet type was calculated using median Cr_2O_3 of garnets (Table 2, equation 1). Other oxides were calculated from Al_2O_3 using equations in Table 2; SiO_2 by difference. Xenolith data sources given in Table 1.

Table 4. SCLM compositions calculated from median garnet composition

Archons	Daldyn Lherz	Daldyn Harz	Kaapvaal Lherz <90Ma	Kaapvaal Harz <90Ma	Kaapvaal Lherz >90Ma	Kaapvaal Harz >90Ma	Malo Bot Lherz	Malo Bot Harz	Alakit Lherz	Alakit Harz
Proportion*	0.68	0.32	0.84	0.16	0.81	0.19	0.83	0.17	0.53	0.47
Garnet Cr_2O_3	4.66	7.90	3.60	5.50	3.90	7.10	4.41	5.55	4.48	7.96
SiO_2	45.8	45.4	46.0	45.7	46.0	45.5	45.8	45.6	45.8	45.4
TiO_2	0.05	0.02	0.07	0.04	0.06	0.02	0.05	0.04	0.05	0.02
Al_2O_3	1.20	0.39	1.73	0.90	1.56	0.52	1.31	0.88	1.28	0.38
Cr_2O_3	0.31	0.18	0.40	0.26	0.37	0.20	0.33	0.26	0.32	0.18
FeO	6.5	6.1	6.8	6.3	6.7	6.2	6.6	6.3	6.5	6.1
MnO	0.11	0.11	0.12	0.11	0.12	0.11	0.11	0.11	0.11	0.11
MgO	44.9	47.2	43.5	45.8	43.9	46.9	44.6	45.8	44.7	47.2
CaO	0.7	0.2	1.0	0.5	0.9	0.3	0.8	0.5	0.8	0.2
Na_2O	0.08	0.03	0.12	0.06	0.11	0.04	0.09	0.06	0.09	0.03
NiO	0.29	0.32	0.27	0.30	0.27	0.31	0.28	0.30	0.28	0.32
Mean comp. (weighted)	Daldyn		Kaapvaal <90 Ma		Kaapvaal >90 Ma		Malo Bot		Alakit	
SiO_2	45.7		46.0		45.9		45.8		45.6	
TiO_2	0.04		0.06		0.05		0.05		0.03	
Al_2O_3	0.94		1.60		1.39		1.24		0.86	
Cr_2O_3	0.27		0.38		0.34		0.32		0.26	
FeO	6.4		6.7		6.6		6.5		6.3	
MnO	0.11		0.12		0.11		0.11		0.11	
MgO	45.7		43.8		44.4		44.8		45.9	
CaO	0.6		1.0		0.8		0.7		0.5	
Na_2O	0.07		0.11		0.10		0.09		0.06	
NiO	0.30		0.27		0.28		0.29		0.30	
atomic ratios										
mg#	92.7		92.1		92.3		92.5		92.8	
Mg/Si	1.49		1.42		1.45		1.46		1.50	
Ca/Al	0.55		0.55		0.55		0.55		0.55	
Cr/Cr+Al	0.16		0.14		0.14		0.15		0.17	
Fe/Al	4.80		2.98		3.36		3.74		5.24	

* Proportions of garnet types (Figure 2A) from GRIFFIN *et al.* (1998a) and authors' unpublished data

change in slope at 2–2.5% Al_2O_3, expressed by two equations for different compositional ranges in Table 2. A scatter of high Ca values in YETI comes mainly from eastern Australia, and reflects amphibole-apatite metasomatism (O'REILLY and GRIFFIN, 1988). The AOP samples show a range of depletion; note that these reconstituted analyses have Ca-Al relationships similar to those of most xenoliths and massifs, which is not true of most bulk analyses of serpentinised abyssal peridotites (Table 1). Kerguelen xenoliths are highly depleted. Archon xenoliths (ARK) are also strongly depleted, but have Ca/Al distinctly lower than the other depleted suites.

FeO. There is no correlation between Fe and Al in the YETI or TILE suites; most FeO contents fall within a narrow range, and some high values are clearly related to metasomatism. The PROT and most MAS data show a weak positive correlation between Fe and Al, while the AOP data show a marked negative correlation. Kaapvaal xenoliths have significantly lower Fe contents at any Al than the other suites, and a positive Fe-Al correlation. As noted above, the Daldyn samples are enriched in Fe by late-stage alteration, and thus are plotted only as medians.

MgO. MgO increases as Al decreases, consistent with melt-depletion models. As with Ca, there is a break in the slope of the correlation at 2–2.5% Al_2O_3, in the YETI and TILE data (see two equations in Table 2). The PROT, ARK and MAS data lie on a steeper trend. Compared to these suites, the AOP data have higher Al for each MgO except in the most depleted samples, which may indicate an overestimation of the modal abundance of spinel.

mg#. The ARK, PROT and MAS samples lie above the linear trend defined by the other data sets; this is partly the effect of the break in slope of the Mg-Al correlation at high degrees of depletion, but also reflects the generally lower Fe at any Al of these

Table 4. (Cont.)

Archons (cont.)	Upper Muna Lherz	Upper Muna Harz	Liaoning Lherz	Liaoning Harz	Shandong Lherz	Shandong Harz	Venezuela Lherz	Venezuela Harz	Slave Lherz	Slave Harz
Proportion*	0.73	0.27	0.8	0.2	0.58	0.42	0.72	0.28	0.73	0.27
Garnet Cr_2O_3	4.35	6.16	6.60	9.80	4.50	8.25	5.78	8.48	6.36	7.37
SiO_2	45.9	45.6	45.5	45.3	45.8	45.4	45.6	45.4	45.6	45.5
TiO_2	0.05	0.03	0.02	0.01	0.05	0.01	0.03	0.01	0.03	0.02
Al_2O_3	1.34	0.71	0.61	0.20	1.27	0.35	0.81	0.32	0.67	0.47
Cr_2O_3	0.33	0.23	0.22	0.15	0.32	0.18	0.25	0.17	0.23	0.20
FeO	6.6	6.3	6.2	6.0	6.5	6.1	6.3	6.1	6.2	6.1
MnO	0.11	0.11	0.11	0.10	0.11	0.11	0.11	0.11	0.11	0.11
MgO	44.6	46.3	46.6	47.7	44.8	47.3	46.0	47.4	46.4	47.0
CaO	0.8	0.4	0.4	0.1	0.8	0.2	0.5	0.2	0.4	0.3
Na_2O	0.09	0.05	0.04	0.01	0.09	0.02	0.06	0.02	0.05	0.03
NiO	0.28	0.31	0.31	0.33	0.28	0.32	0.30	0.32	0.31	0.32
Mean comp. (weighted)	Upper Muna		Liaoning		Shandong		Venezuela		Slave	
SiO_2	45.8		45.5		45.6		45.6		45.5	
TiO_2	0.05		0.02		0.04		0.03		0.02	
Al_2O_3	1.17		0.53		0.88		0.68		0.61	
Cr_2O_3	0.31		0.21		0.26		0.23		0.22	
FeO	6.5		6.2		6.3		6.2		6.2	
MnO	0.11		0.11		0.11		0.11		0.11	
MgO	45.0		46.8		45.8		46.4		46.6	
CaO	0.7		0.3		0.5		0.4		0.4	
Na_2O	0.08		0.04		0.06		0.05		0.04	
NiO	0.29		0.31		0.30		0.31		0.31	
atomic ratios										
mg#	92.5		93.1		92.8		93.0		93.1	
Mg/Si	1.47		1.54		1.50		1.52		1.53	
Ca/Al	0.55		0.55		0.55		0.55		0.55	
Cr/Cr+Al	0.15		0.21		0.17		0.19		0.19	
Fe/Al	3.94		8.22		5.10		6.54		7.17	

samples, especially those from Archons. YETI points scattering to low mg# are mainly metasomatised samples from eastern Australia, while those from the TILE set are mainly from Dreiser Weiher. The Gnt-SCLM data for Protons have generally higher mg# at each Al than the spinel-peridotite data shown by the PROT medians.

SiO_2. SiO_2 and Al_2O_3 are positively correlated in all sets, reflecting the general increase in Mg/Si characteristic of depletion and increasing olivine enrichment in the residue. However, the medians and the Gnt-SCLM lines show a progression in the slope and position (mean Si/Al) of the correlation from YETI to PROT to ARK, which does not correlate simply with degree of depletion.

Cr_2O_3. There is no overall correlation between Cr and Al in the YETI or TILE suites. The PROT and MAS samples show a weak positive correlation, while the ARK samples show marked depletion in Cr and a strong positive Cr-Al correlation (see equations in Table 2). The AOP data show high Cr values and a good positive correlation between Cr and Al; both are interpreted by us as artefacts, resulting from a small overestimation of the modal abundance of spinel. Whole-rock analyses of abyssal peridotites (Table 1) show Cr contents comparable to those of YETI or TILE xenoliths, and no obvious Cr-Al correlation. Strongly depleted OPH rocks have relatively high Cr contents (Table 1).

TiO_2. The Ti data define a broad positive correlation that intersects the Al_2O_3 axis at ≈0.5%. Taking this correlation as the general depletion trend, it seems probable that many ARK xenoliths have had TiO_2 added by metasomatism at some time after their initial depletion. Amphibole-bearing samples from Dreiser Weiher and eastern Australia show high Ti/Al compared to the main trend of YETI and TILE data.

Na_2O. Most of the data define a broad positive correlation, with a trend that intersects the Al_2O_3 axis

Table 4. (Cont.)

Protons	Merchimden	U. Molodo	Kuoika	Guizhou	Hubei	Arkansas	S. Australia	Ellendale	Color. Plat.	Argyle	Argyle
Garnet Cr_2O_3	2.80	2.76	3.14	3.33	2.18	2.66	3.38	4.25	2.12	3.88	
SiO_2	44.8	44.8	44.6	44.5	45.3	44.9	44.4	44.0	45.4	44.2	45.9
TiO_2	0.09	0.09	0.08	0.08	0.11	0.10	0.07	0.06	0.12	0.06	0.06
Al_2O_3	2.3	2.3	2.0	1.9	2.8	2.4	1.9	1.4	2.9	1.6	1.6
Cr_2O_3	0.42	0.42	0.42	0.41	0.43	0.42	0.41	0.40	0.43	0.41	0.37
FeO	7.9	7.9	7.8	7.8	8.0	7.9	7.8	7.7	8.0	7.7	6.7
MnO	0.13	0.13	0.13	0.13	0.13	0.13	0.13	0.13	0.13	0.13	0.12
MgO	41.9	41.8	42.7	43.1	40.2	41.6	43.2	44.7	40.1	44.1	43.9
CaO	2.0	2.0	1.8	1.7	2.5	2.1	1.6	1.2	2.5	1.4	1.0
Na_2O	0.16	0.16	0.14	0.13	0.20	0.17	0.13	0.10	0.20	0.11	0.11
NiO	0.29	0.28	0.29	0.30	0.27	0.28	0.30	0.32	0.26	0.31	0.29
atomic ratios											
mg#	90.5	90.4	90.7	90.8	90.0	90.4	90.8	91.2	89.9	91.1	92.1
Mg/Si	1.40	1.39	1.43	1.45	1.33	1.38	1.45	1.52	1.32	1.49	1.43
Ca/Al	0.80	0.80	0.80	0.80	0.80	0.80	0.80	0.80	0.80	0.80	0.59
Cr/Cr+Al	0.11	0.11	0.12	0.13	0.09	0.11	0.13	0.16	0.09	0.15	0.14
Fe/Al	2.45	2.42	2.74	2.91	2.01	2.34	2.96	3.95	1.97	3.49	3.02

Tectons	Vitim	E. China	Taihang	Tieling	Mt. Horeb	Malaita	W. Cliffs	Renmark	Jugiong
Garnet Cr_2O_3	1.5	1.3	1.81	2.2	1.4	1.3	1.91	1.46	1.67
SiO_2	44.5	44.5	44.5	44.5	44.5	44.5	44.5	44.5	44.5
TiO_2	0.15	0.15	0.13	0.11	0.15	0.15	0.12	0.14	0.13
Al_2O_3	3.7	3.8	3.2	2.8	3.7	3.8	3.1	3.6	3.4
Cr_2O_3	0.40	0.40	0.40	0.40	0.40	0.40	0.40	0.40	0.40
FeO	8.0	8.0	8.0	8.0	8.0	8.0	8.0	8.0	8.0
MnO	0.13	0.13	0.13	0.13	0.13	0.13	0.13	0.13	0.13
MgO	39.3	39.1	40.2	41.0	39.3	39.1	40.4	39.5	39.9
CaO	3.3	3.4	2.9	2.6	3.3	3.4	2.8	3.2	3.0
Na_2O	0.26	0.27	0.22	0.20	0.26	0.27	0.22	0.25	0.24
NiO	0.25	0.25	0.26	0.27	0.25	0.25	0.26	0.25	0.26
atomic ratios									
mg#	89.8	89.7	90.0	90.1	89.8	89.7	90.0	89.8	89.9
Mg/Si	1.32	1.31	1.35	1.37	1.32	1.31	1.36	1.33	1.34
Ca/Al	0.81	0.80	0.83	0.85	0.81	0.80	0.83	0.81	0.82
Cr/Cr+Al	0.07	0.07	0.08	0.09	0.07	0.07	0.08	0.07	0.07
Fe/Al	1.53	1.48	1.77	2.02	1.53	1.48	1.83	1.57	1.68

at ≈1%. A number of samples with markedly high Na/Al show modal metasomatism, usually with amphibole present. The moderate Na contents of the ARK xenoliths also may reflect metasomatism.

Element ratios vs mg#

Key element ratios (atomic ratios) are plotted against mg# (100 Mg/(Mg + Fe) in Fig. 4; the layout is similar to that of Fig. 3.

cr#. The YETI and TILE xenoliths define a well-constrained field, with a sharp lower boundary; this reflects the relatively constant Cr in these suites over a wide range of Al contents. The PROT and MAS data are similar, but scatter more widely; the ARK data, especially for the Gnt-SCLM compositions, extend to higher mg# without a corresponding increase in cr#. The AOP data show a vertical distribution, probably reflecting the spinel-overestimation problem noted above.

Mg/Si. In the YETI and TILE suites, Mg/Si (atomic ratio) shows a general increase with degree of depletion as measured by mg#, corresponding to the "oceanic trend" of Boyd (1989). The least depleted xenoliths are similar to the composition of Primitive Upper Mantle (PUM) as estimated by McDonough and Sun (1995) but the main trend of the data would suggest a slightly higher Mg/Si (≥1.3) at the corresponding mg#. A similar trend is shown by the PROT and MAS data, but it is displaced to higher mg#. The ARK set is displaced to still higher mg#, without a corresponding increase in Mg/Si.

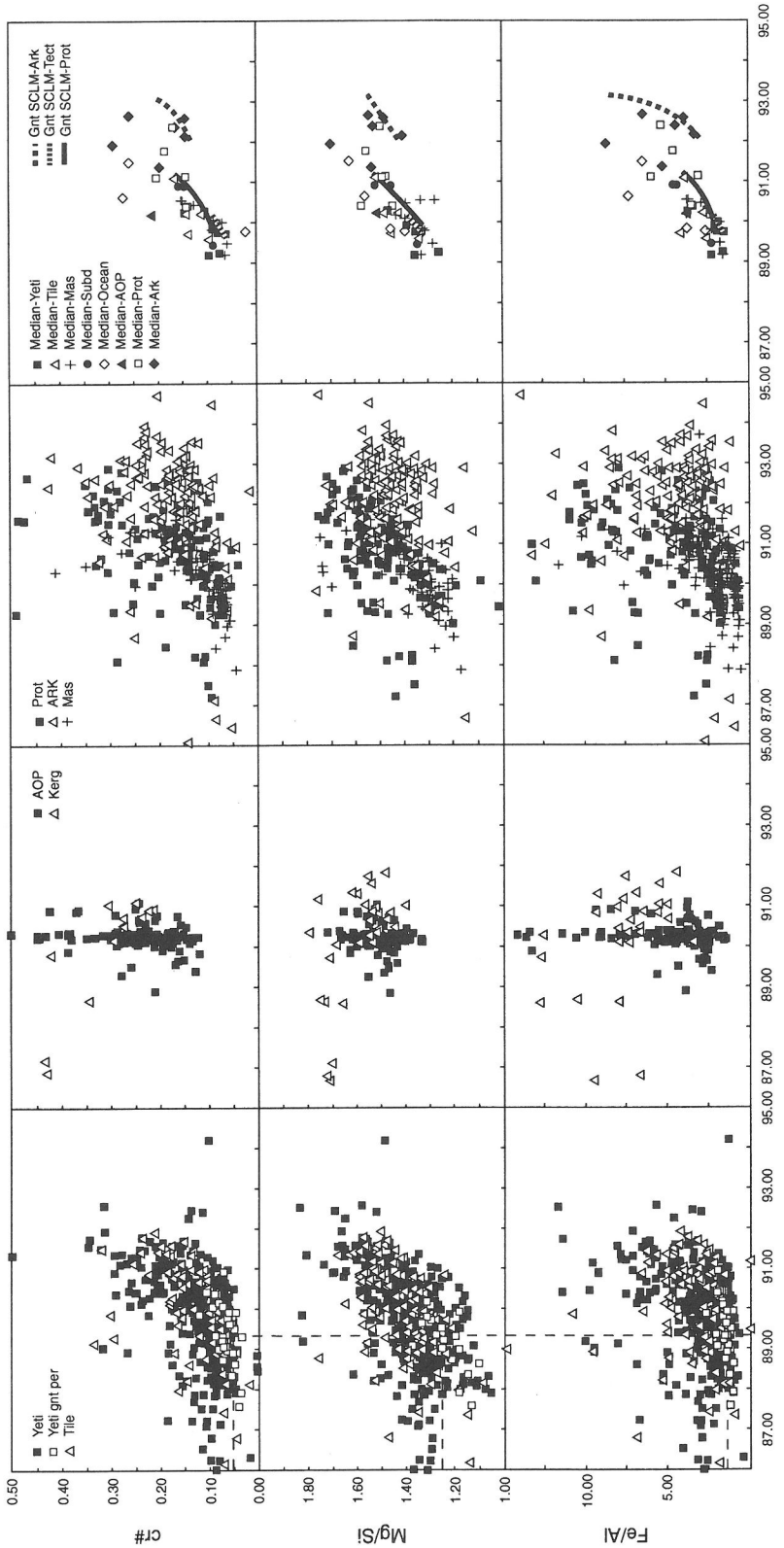

FIG. 4. Atomic ratios plotted against mg# (=100Mg/(Mg + Fe)). cr# = atomic Cr/(Cr + Al). Other symbols and data sets as in Fig. 3.

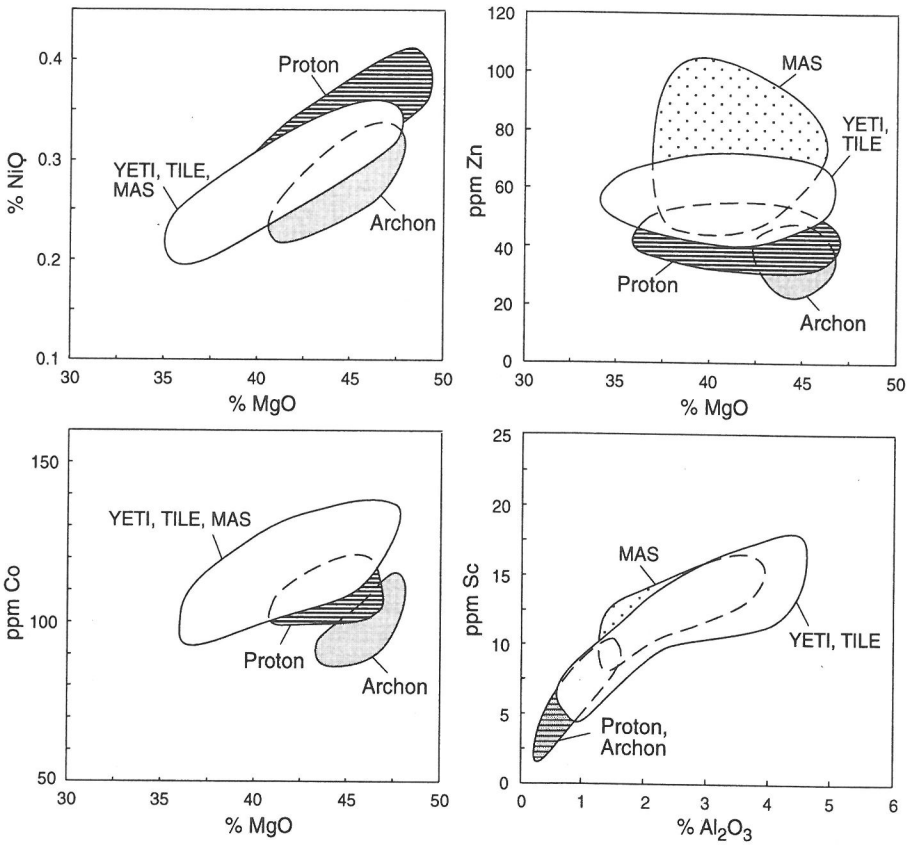

FIG. 5. NiO, Co, Zn and Sc contents plotted against MgO and Al_2O_3 (fields only).

Fe/Al. Mean and minimum values of Fe/Al (atomic ratio) rise slowly with increasing mg# in the YETI and TILE data sets. The PROT and MAS data show a steeper trend, but the ARK samples, although more depleted on average (higher mg#) have low Fe/Al.

Minor elements

Data for several compatible minor elements, which we regard as insensitive to metasomatism, are shown in Fig. 5. Ni and Mg are well-correlated in most of the data sets, but the ARK data, as well as those from Kerguelen and Lanzarote, lie below this trend. Zn shows a weak negative correlation with MgO in most data sets, but the MAS data show a larger scatter, which may be related to metasomatic processes. PROT samples have lower mean Zn than YETI, TILE or MAS, and ARK samples have still lower Zn. V (not shown) also is negatively correlated with MgO. Co contents rise slowly with increasing MgO in all of the data sets except ARK (data only from Siberia), where Co contents are significantly lower than in the other sets and well-correlated with MgO. Sc shows a good positive correlation with Al_2O_3; the slope of the trend is moderate at low degrees of depletion, and steepens sharply below $\approx 2\%$ Al_2O_3, suggesting that Sc becomes more incompatible at high degrees of depletion, as cpx and gnt disappear from the residue.

DISCUSSION

The composition of SCLM

The data derived from xenoliths and garnet concentrates may not be representative of the whole lithosphere section in any given locality. The more abundant garnet data show considerable vertical variation in rock-type distribution between cratons and even between different terranes or time intervals within single cratons (Fig. 6). In Tecton areas, the deeper garnet-bearing peridotites are generally less depleted than the shallow spinel peridotites (Tables 1, 5). However, by considering enough different areas,

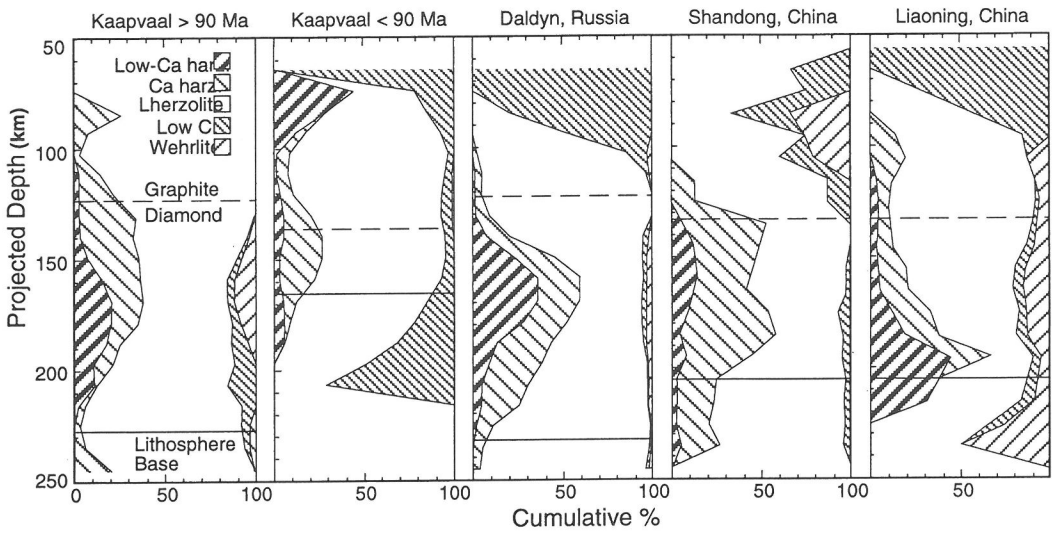

FIG. 6. Sections showing depth distribution of mantle rock types, derived from proportions of garnet xenocryst types as defined in Fig. 2A. Depth for each garnet grain was derived by extrapolating its Nickel Temperature (GRIFFIN *et al.*, 1989a) to the local geotherm (RYAN *et al.*, 1996). Lithosphere base represents deepest extent of Y-depleted ($Y \leq 10$ ppm) garnets (GRIFFIN and RYAN, 1995). Two time slices are shown for the Kaapvaal Craton, based on kimberlites intruded before and after 90 Ma; thermal erosion and metasomatism by asthenosphere-derived melts around 90 Ma has removed 40–60 km of the lithosphere and reduced the abundance of harzburgite (GRIFFIN *et al.*, 1995). The section for the Daldyn kimberlite field (Siberian Platform; after GRIFFIN *et al.*, 1996) includes data from the Udachnaya kimberlite pipe. Shandong and Liaoning sections represent two terranes within the Sino-Korean Craton of NE China (GRIFFIN *et al.*, 1998b).

we can hope to construct meaningful average compositions for different types of mantle volumes.

The Gnt-SCLM data for Archon sections (Table 4) agree well with xenolith data where these are available (Table 3). The mean compositions calculated for ten Archon sections worldwide (Table 4) show a wide range, but all are highly depleted and have compositions consistent with xenolith data in terms of individual elements and important ratios (Fig. 7). We therefore regard the mean Archon Gnt-SCLM (Table 5) as the best available estimate for the mean composition of Archean lithospheric mantle. In terms of Ca and Al contents, this estimate lies between the median values for xenoliths from the Kaapvaal and Daldyn areas; its mg# is higher than either xenolith set, but as noted above, the analysed mg# for the Daldyn xenoliths has been lowered by late metasomatism (BOYD *et al.*, 1997). The few data for xenoliths from the Slave craton of northern Canada (PEARSON *et al.*, 1998; authors' upubl. data) are derived from modal analysis of small (1–2 cm) xenoliths, which may represent a biased selection of olivine-rich rocks, but the Gnt-SCLM data for the Slave craton also suggest a highly depleted composition.

The "Gnt-SCLM" estimates for each of ten Proton sections (Table 4) also show a wide range in Ca and Al, which overlaps at the low end with the data from Archons. The most depleted sections, Argyle and Ellendale, intrude Proterozoic mobile belts, but the lamproites contain rare diamonds of harzburgitic paragenesis (JAQUES *et al.*, 1989) and these sections could represent modified Archon lithosphere. None of these estimates is as depleted as the median Namibian xenolith composition (Table 1), and the mean Gnt-SCLM for Protons is less depleted than the mean of the limited xenolith data, some of which may be biased by exclusion of abundant pyroxenitic variants (see above). The weighted median of the MAS data (Table 5) is similar to the median Proton Gnt-SCLM, and this is consistent with Proterozoic Re-Os depletion ages on several of the European orogenic massifs (REISBERG and LORAND, 1995; MEISEL *et al.*, 1996a). A mean of these three values therefore may give the best available estimate of Proton SCLM composition (Table 5, "preferred").

The mean TILE xenolith composition is very similar to the mean Proton SCLM composition. We suggest that the TILE xenolith suites consist largely of remnant older (Proterozoic?) mantle, with a smaller proportion of younger YETI-type material. This is consistent with Proterozoic Re-Os depletion

Table 5. Estimates of mean SCLM composition

ARCHONS							PROTONS			
	Av. Archon Gt SCLM (preferred)	Av. Kaapvaal xenoliths	Av. Daldyn xenoliths	Av. Slave xenoliths	Kaapvaal High-T		Av. Proton Gt SCLM	Av. Proton xenoliths	Av. Massif	Proton SCLM (preferred)
SiO_2	45.7	46.5	43.7	42.9	44.3	SiO_2	44.7	43.9	45.2	44.6
TiO_2	0.04	0.06	0.05	0.0	0.17	TiO_2	0.09	0.04	0.09	0.07
Al_2O_3	0.99	1.40	0.92	1.1	1.74	Al_2O_3	2.1	1.6	2.0	1.9
Cr_2O_3	0.28	0.34	0.37	0.5	0.30	Cr_2O_3	0.42	0.40	0.38	0.40
FeO	6.4	6.6	7.5	7.2	8.1	FeO	7.9	7.9	7.9	7.9
MnO	0.11	0.10	0.12	0.1	0.12	MnO	0.13	0.12	0.11	0.12
MgO	45.5	43.8	46.0	47.2	43.3	MgO	42.4	43.9	41.6	42.6
CaO	0.59	0.88	0.94	0.6	1.27	CaO	1.9	1.3	1.9	1.7
Na_2O	0.07	0.10	0.07	0.0	0.12	Na_2O	0.15	0.08	0.13	0.12
NiO	0.30	0.29	0.30	0.31	0.26	NiO	0.29	0.22	0.28	0.26
Zn, ppm	34	44	34			Zn, ppm	45	42	70	52.33
V, ppm	20	28	25		26	V, ppm	40	37	68	48.33
Co, ppm	93	93	93			Co, ppm	105	106	111	107.33
Sc, ppm	7	6	7			Sc, ppm	10	7	13	10.00
atomic ratios						*atomic ratios*				
mg#	92.7	92.3	91.7	92.1	90.5	mg#	90.6	90.8	90.4	90.6
Mg/Si	1.49	1.41	1.57	1.64	1.46	Mg/Si	1.42	1.49	1.38	1.43
Ca/Al	0.55	0.57	0.93	0.50	0.67	Ca/Al	0.80	0.73	0.87	0.80
Cr/Cr+Al	0.16	0.14	0.21	0.23	0.10	Cr/Cr+Al	0.12	0.15	0.11	0.12
Fe/Al	4.66	3.36	5.83	4.71	3.37	Fe/Al	2.64	3.66	2.78	3.02
ol/opx/cpx/gt	69/25/2/4				70/18/4/8	ol/opx/cpx/gt				70/17/6/7
density, g/cc	3.31				3.36	density, g/cc				3.34
Vp, km/s(room)	8.34				8.33	Vp, km/s (room)				8.32
Vp, 50km,400°C	8.18					Vp, 50km,500°C				8.10
Vp, 100km,700°C	8.18					Vp, 100km,900°C				8.05
Vs, km/s(room)	4.88				4.85	Vs, km/s(room)				4.84
Vs, 50km,400°C	4.76					Vs, 50km,500°C				4.69
Vs, 100km,700°C	4.71					Vs, 100km,900°C				4.60

ages on xenoliths from the Eifel (COHEN *et al.*, 1996; MEISEL *et al.*, 1996b).

It is more difficult to estimate a mean composition for Tecton SCLM, because two different types of material are represented. The Tecton Gnt-SCLM is essentially identical to the mean Tecton garnet peridotite, and to the Zabargad spinel peridotites (Table 5). This material may give the best estimate of the composition of SCLM being generated in areas of extension during Cenozoic time. It is less depleted than the mean YETI xenolith composition, and only mildly depleted compared to estimates (Table 5) of primitive mantle and MORB-source compositions by JAGOUTZ *et al.* (1979), ALLEGRE *et al.* (1995) and NIU (1997). In general YETI shows less depletion than TILE or MAS; many YETI spinel-peridotite xenoliths can be modelled as the result of ≈5% batch melting from a PUM source (NORMAN, 1998; XU *et al.*, 1998), and many YETI garnet peridotites (and Zabargad) are even less depleted (Table 1, Fig. 3). Many of the YETI xenolith suites may consist of a mixture of fertile Phanerozoic material and more depleted older material, but weighted toward the former, in contrast to the TILE suites.

An estimate of the composition of SCLM beneath areas of Phanerozoic crust (as defined by the last major tectonothermal event) would have to evaluate the relative proportions of these different suites, which would require a tectonic analysis outside the scope of this work. However, a useable overall estimate may be given by the median YETI spinel peridotite suite (Table 5); this is slightly less depleted than the averages of spinel lherzolite xenoliths from a range of environments, given by MCDONOUGH (1990; Table 5) or MAALØE and AOKI (1977).

Secular evolution of SCLM composition: crust-mantle linkages

The abundant data on garnet compositions (GRIFFIN *et al.*, 1998a,c; Table 4) show that subcalcic (*i.e.* cpx-free) garnet harzburgites (as defined by their garnet composition, Fig. 2A) are restricted, with rare exceptions, to Archon SCLM. The garnet data (Fig. 2B) and

Table 5. (cont.)

	TECTONS					MODELS				
	Av. Tecton gt SCLM	Av. YETI gt per.	Zabargad spinel per.	Av. YETI spinel per. (preferred)	Av. TILE spinel per.	Prim. Mantle MS(1995)	Prim. Mantle J(1979)	MORB N(1997)	PRIMA A(1995)	Av. Spin. Per. Xens. M(1990)
SiO_2	44.5	45.0	44.3	44.4	44.4	45.0	45.2	45.5	46.1	44.0
TiO_2	0.14	0.16	0.11	0.09	0.09	0.20	0.22	0.16	0.18	0.09
Al_2O_3	3.5	3.9	3.9	2.6	1.8	4.5	4.0	4.2	4.1	2.3
Cr_2O_3	0.40	0.41	0.38	0.40	0.39	0.38	0.46	0.45	0.38	0.39
FeO	8.0	8.1	8.5	8.2	8.3	8.1	7.8	7.7	7.5	8.4
MnO	0.13	0.07	0.14	0.13	0.14	0.14	0.13	0.13	0.15	0.14
MgO	39.8	38.7	39.2	41.1	42.7	37.8	38.3	38.3	37.8	41.4
CaO	3.1	3.2	3.1	2.5	1.8	3.6	3.5	3.4	3.2	2.2
Na_2O	0.24	0.28	0.35	0.18	0.16	0.36	0.33	0.3	0.36	0.24
NiO	0.26	0.24	0.26	0.27	0.28	0.25	0.27	0.26	0.25	0.26
Zn, ppm	55	56		53	65	55	50			65
V, ppm	70	58	54	59	67	82	77			56
Co, ppm	110	102	108	110	104	105	105			112
Sc, ppm	14	14	12	12	13	16	17			12
atomic ratios						*atomic ratios*				
mg#	89.9	89.5	89.2	89.9	90.2	89.3	89.7	89.9	90.0	89.8
Mg/Si	1.33	1.28	1.32	1.38	1.44	1.25	1.27	1.26	1.22	1.41
Ca/Al	0.82	0.76	0.71	0.85	0.90	0.73	0.81	0.74	0.72	0.86
Cr/Cr+Al	0.07	0.07	0.06	0.09	0.13	0.05	0.07	0.07	0.06	0.10
Fe/Al	1.66	1.50	1.56	2.23	3.31	1.30	1.42	1.32	1.32	2.67
ol/opx/cpx/gt	60/17/11/12			66/17/9/8		57/13/12/18				
density, g/cc	3.37			3.36		3.39				
Vp, km/s(room)	8.30			8.30		8.33				
Vp 50km,800°C	7.86			7.86						
Vp 100km,1200°C	7.85			7.85						
Vs, km/s(room)	4.82			4.82		4.81				
Vs 50km,800°C	4.52			4.52						
Vs 100km,1200°C	4.48			4.48						

Notes: Modes calculated using average compositions for minerals from rocks of similar composition. Density, Vp and Vs calculated using modes, mineral compositions and end-member data as discussed in text. References: MS(1995), McDonough and Sun (1995); J(1979), Jagoutz *et al.* (1979); N(1997), Niu (1997); A(1995), Allegre *et al.* (1995); McDonough (1990).

the Gnt-SCLM data (Tables 4 and 5) also show that the median composition of SCLM garnet lherzolites has changed with time, from extreme depletion in the Archon suites (*e.g.*, $\leq 1\%$ Al_2O_3) to lower degrees of depletion in Proton suites ($Al_2O_3 \approx 2\%$) to still less depletion in Tecton suites ($Al_2O_3 \geq 3\%$). This secular trend toward lower degrees of depletion is clear even if the YETI spinel peridotites, rather than the Tecton garnet peridotites or the Zabargad spinel peridotites, are regarded as the most typical Phanerozoic SCLM.

Several of the important differences between Archon, Proton and Tecton SCLM are illustrated in Fig. 7. The Archon xenoliths (both lherzolites and harzburgites) and Gnt-SCLM compositions consistently lie off the trends defined by the Proton and Tecton data. Considering its high degree of depletion (high mg#), the Archon SCLM has anomalously low FeO contents, Mg/Si, Fe/Al and cr#; it also has anomalously low Ni, Zn and Co contents (Fig. 5). O'Hara *et al.* (1975) recognised several of these major-element differences between xenoliths in kimberlites (Archons) and xenoliths in alkali basalts (Tecton), and these differences were defined in more detail by Boyd (1989, 1997a). This work extends those observations to a larger data set, defines the transitional nature of Proton SCLM, and emphasises the fertile nature of more recently formed Tecton SCLM, as represented by Tecton garnet peridotite xenoliths or even the YETI spinel peridotite xenoliths (Table 5).

These data imply a fundamental change in SCLM-forming processes between Archean and Proterozoic time, and an evolution in process through post-Archean time, leading to progressively less-depleted mean SCLM compositions. Mechanisms for producing this evolution are discussed below. The correlation of SCLM composition with the tectonothermal age of the overlying crust further implies that crustal volumes generally have been formed quasi-

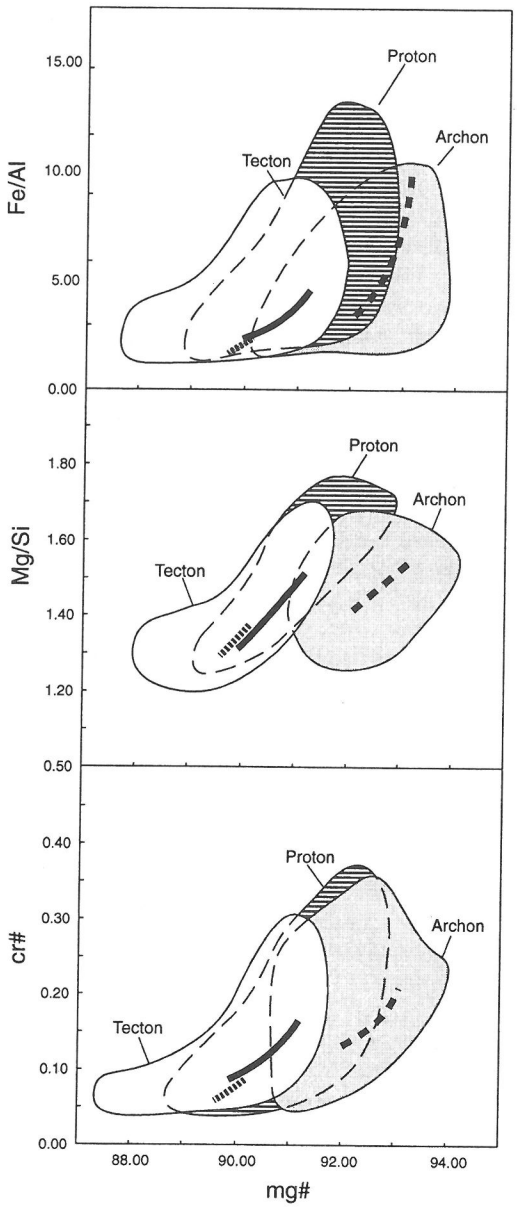

FIG. 7. Fields of atomic Fe/Al, Mg/Si and cr# (=Cr/(Cr + Al)) vs mg#, for Archon, Proton and Tecton xenoliths. Ornamented lines show Garnet-SCLM ranges for each type, from Table 4.

contemporaneously with their underlying SCLM, and that the crust and the SCLM can stay coupled together, for timespans measured in aeons.

This conclusion does not relate only to continent-scale volumes, but can be extended to individual crustal volumes on the scale of individual terranes, with dimensions of several hundred kilometres. Such terranes have been shown to have distinctively different mantle stratigraphy within the Sino-Korean craton (Fig. 6; GRIFFIN *et al.*, 1998b) and the Siberian craton (GRIFFIN *et al.*, 1996, 1998d). This implies that relatively small crustal volumes have been able to retain their own SCLM during and after the processes that assembled them into larger cratons. Further analysis will be required to understand the differences in process that have produced the large differences in rock-type stratigraphy among Archean mantle sections (Fig. 6).

The origin of Archean SCLM

In the Gnt-SCLM data from Archon sections, the median Cr content of harzburgitic garnets is correlated with the median Cr contents of lherzolite garnets, and with the relative abundance of such garnets in the section (Fig. 8). These relationships imply that the lherzolites and the harzburgites are linked by a common depletion process. Detailed modal and mi-

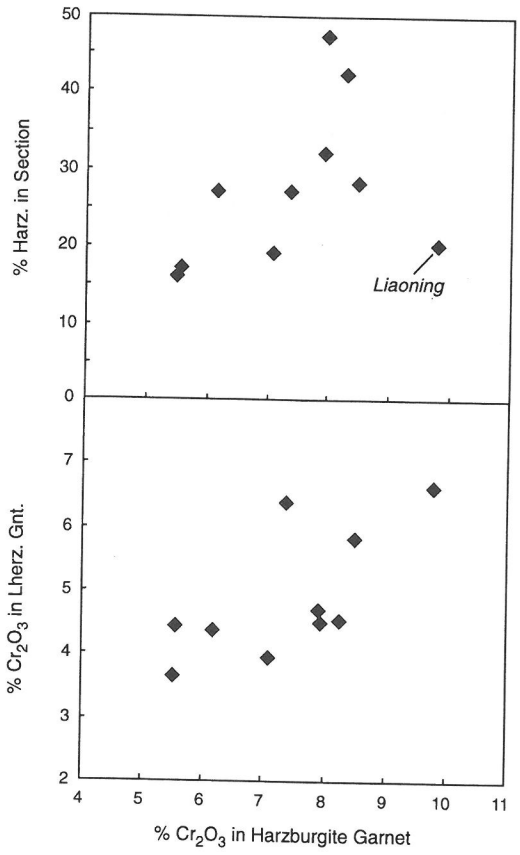

FIG. 8. Relationships between median Cr_2O_3 content of harzburgitic and lherzolitic garnets, and harzburgite abundance (as estimated from garnet concentrates), for the Archon sections shown in Table 4. Data from GRIFFIN *et al.* (1998a; Table 1).

crostructural analysis of granular xenoliths (Cox *et al.*, 1987) suggests that most, if not all, of the cpx and garnet in Kaapvaal lherzolites and harzburgites exsolved from complex magmatic orthopyroxenes during cooling from igneous temperatures; this interpretation has been supported by experimental studies (Canil, 1991; 1992).

The compositional data given here also are consistent with this model. The apparently incompatible nature of both Cr and Sc at high degrees of depletion (low Al contents) in the Archon xenoliths suggests that no Cr-Al phase (garnet or spinel) was present in the residue during the depletion event, and that clinopyroxene (the other main host, with garnet, for Sc) also was absent. The break in slope of the Ca-Al and Mg-Al depletion trends at ≈2.5% Al_2O_3 (Fig. 3) may reflect the disappearance of cpx from the residue. The total range in mg# of the Garnet-SCLM estimates for Archons is only 1%, while the median concentrations of CaO and Al_2O_3 vary by a factor of three. More strongly depleted SCLM also may be more strongly differentiated. In sections with a high abundance of harzburgitic garnets, such garnets tend to be more strongly concentrated in specific depth ranges (Table 4, Fig. 6). All of these features are consistent with some form of sorting between olivine and high-T complex orthopyroxenes, as suggested by Boyd (1989; 1997b) and Herzberg (this volume).

Herzberg (this volume) has suggested that such sorting might take place during melting at considerable depth. The argument for melting at high pressures is strengthened by the low Ni/Mg, Zn/Mg and Co/Mg of the Archon xenoliths, compared to those from Proton and Tecton settings (Fig. 5). Bickle *et al.* (1977) showed that $D_{Ni}^{(oliv/melt)}$ decreases with increasing pressure, such that high-P residues will be depleted in Ni; Suzuki and Akogi (1995) confirmed this result for Ni and extended it to other divalent elements such as Co and Zn.

Many authors (from O'Hara *et al.*, 1975) have suggested that the depletion of Archean SCLM is related to the extraction of komatiitic magmas at high P. One problem with this model has been the failure of experimental studies to produce the subcalcic Cr-rich garnets characteristic of Archean harzburgites (Canil and Wei, 1992). However, this argument seems to require that the garnet should be a residual phase; if the garnet is a subsolidus reaction product, as discussed above, this is not a valid objection. Another problem relates to the low Mg/Si of Archean SCLM. Komatiitic magmas have SiO_2 contents (46–49%) higher than those of pyrolite or primitive mantle (45–46%), and the extraction of komatiites therefore will leave a residue depleted in SiO_2. Walter (1997) has shown that komatiite extraction from a pyrolite mantle at high P can produce residues similar to the Daldyn xenolith suite, but that a more Si-rich mantle composition would be required to produce the Kaapvaal xenolith suite by komatiite extraction. However, the lower Si contents of the Daldyn xenoliths are largely a secondary effect, reflecting late-stage metasomatic enrichment in Fe and Ca (Boyd *et al.*, 1997). When compositions calculated from modal data or garnet data (Boyd *et al.*, 1997; Tables 3, 4) are used, the Si contents and Mg/Si of Daldyn and Kaapvaal xenoliths are similar, and the problem associated with a komatiite-extraction model remains.

Kelemen and coworkers (Kelemen *et al.*, 1992; Kelemen and Hart, 1996; Kelemen and Bernstein, 1997) have suggested that the high Si contents of the Archean SCLM reflect metasomatism by felsic magmas such as trondhjemites, derived from subducted and melted oceanic crust. However, it is not clear why such Mg/Si relationships should be confined mainly to Archean material, when the suggested plate-tectonic process operates in modern time, and presumably did so back at least into the Proterozoic. The introduction of Si from trondhjemitic melts does not appear to explain the low Fe, Ti, Na, K and Cr of the Archon SCLM. If the Archon SCLM is regarded as the residue of komatiite extraction, then Walter's (1997) data require that the high Si/Mg of Archon mantle was present at least 3.5 Ga ago, and did not develop over a long post-Archean history.

In the felsic-metasomatism model, the more olivine-rich xenoliths represent the least-modified material, and the orthopyroxene-rich xenoliths are most strongly metasomatised. However, if lherzolites and harzburgites are considered separately (Fig. 9), it is seen that the most olivine-rich samples generally have the lowest mg#; they also have the lowest Ni contents (Fig. 5). This is in contrast to younger garnet-peridotite xenolith suites, where the most olivine-rich samples have the highest mg# and Ni contents. The olivine-mg#-Ni relationships of the Archean xenoliths are thus similar to those seen in abyssal peridotites, where they have been modelled (Niu and Hekinan, 1997) as the result of interaction between residues and mafic melts. We suggest that the olivine-orthopyroxene ratios of the Kaapvaal and Daldyn xenoliths reflect percolation of basic or ultrabasic melts through residual or cumulate orthopyroxene-rich rocks, with higher degrees of melt interaction leading to higher proportions of olivine, lower mg# and lower Ni contents. Combined with lower-T redistribution of Ni between olivine and opx, this mechanism can produce the negative correlation between olivine abundance and the Ni content of olivine, seen in many Archon xenoliths (Kelemen and

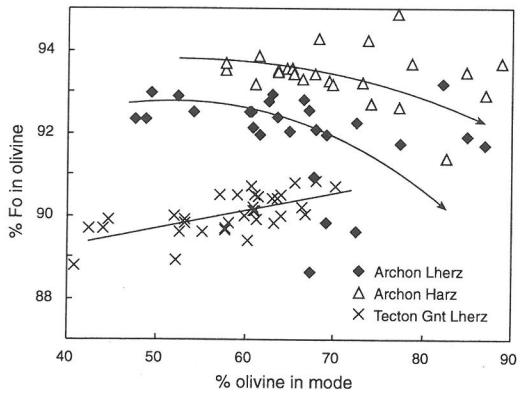

FIG. 9. Relationship between modal olivine content and Fo content of olivine, for depleted Archean lherzolite and harzburgite xenoliths, and for fertile garnet lherzolites from Tectons. Lower curved arrow is drawn as running mean through lherzolite data; upper arrow is for harzburgites. The line through the Tecton xenoliths is interpreted as a depletion trend; the arrows through the Archean data are interpreted as the result of melt retention, leading to more olivine-rich rocks with lower mg#.

BERNSTEIN, 1997; BOYD, 1997b; HERZBERG, this volume).

SCHULZE (1986) has argued that the low Ca contents and Ca/Al ratios of the Archean xenoliths are evidence that these rocks originated as serpentinised oceanic lithosphere, and were subducted to form the continental roots. One main objection to this model is that it does not explain the restriction of subcalcic harzburgites to the Archean, nor the low Mg/Si of the Archean SCLM. In addition, the major-element data show that oceanic lithosphere (as sampled at the surface) is distinct from Archon lithosphere in terms of Fe contents, mg#, cr# and Ca/Al (Table 1). Similarly, while highly depleted peridotites are produced at convergent margins (Table 1), these do not have the low Cr and Fe contents, nor the low Mg/Si and Fe/Al, of Archon xenoliths, and do not provide a realistic analog for the generation of Archean SCLM (cf MENZIES, 1991).

Origin of post-Archean SCLM

Young SCLM might be added to the continents by two basic mechanisms: lateral accretion of material from convergent continental margins (either subducting oceanic lithosphere or material from the mantle wedge above Benioff zones), or underplating by material rising from below. The data in Table 1 and Figs. 3–4 allow some evaluation of these models.

Most xenoliths and dredged peridotites from convergent-margin settings, and the tectonite zones of convergent-margin ophiolites, are significantly more depleted in terms of Ca and Al than the YETI or TILE xenolith suites [Table 1; see compilations by BLOOMER (1983), DICK *et al.* (1984), BONATTI and MICHAEL (1989) and MENZIES (1991)]. Despite their similar mg#, they typically have lower median Ca/Al and higher Fe/Al than YETI or TILE. It is therefore difficult to identify SCLM xenolith suites that could represent accreted convergent-margin upper mantle, although individual xenoliths can be found to match some oceanic rocks.

The abyssal peridotites show a wide range in depletion, related to spreading rate (DICK *et al.*, 1984; BOUDIER and NICOLAS, 1985; NIU and HEKINEN, 1996; NIU, 1997). The more highly depleted AOP of the Pacific are unlike the YETI, TILE and MAS samples that are derived directly from the SCLM. The Atlantic AOP are generally less depleted, thus more similar to, for example, the TILE xenolith suite. However, whole-rock analyses of the actual serpentinised peridotites, as contrasted to the recalculated analyses used here, also show aberrant Ca-Al-Fe relationships that are distinct from those found in most of the Phanerozoic xenolith suites (Table 1). The ophiolites of the Internal Ligurides, believed to be of AOP origin (ERNST, 1978; ERNST and PICCARDO, 1979), have much lower Ca/Al, despite high median Al, than the YETI, TILE or MAS data (Table 1).

It is possible that abyssal-peridotite material exists beneath the Phanerozoic parts of the continents, but has been so modified by metasomatism as to be unrecognisable in xenolith suites. However, such metasomatism would have to restore Ca-Al-Fe relationships destroyed during sea-floor serpentinisation, which seems unlikely. Alternatively, previously serpentinised peridotites might make up only a small part of the accreted material, thus remaining unrecognised in the xenolith suites. However, it is unclear how large volumes of subducted oceanic lithosphere could accrete to form the SCLM without also involving the mantle-wedge material of the active continental margins as well. 3-D seismic mapping of actively subducting oceanic slabs (GUDMUNDSSON and SAMBRIDGE, 1998) shows that these are descending into the upper mantle at relatively steep angles, suggesting that oceanic material is not currently accreting to the SCLM of the younger parts of the continents.

The above arguments also apply to Proton SCLM; the absence of SCLM material that clearly is derived from convergent margins makes it difficult to argue for accretion of oceanic material into the SCLM, even if shallower subduction angles are invoked. While BOYD (1989) and MENZIES (1991) have used the relationships shown in Fig. 1 to suggest that circumcratonic SCLM is similar to oceanic litho-

sphere, the data presented here suggest that there are real differences, and that Phanerozoic SCLM is not simply subducted MORB mantle (cf MENZIES, 1991). The message of Fig. 1 may instead be that both types of material represent melt extraction at relatively shallow depths, without constraint on tectonic setting (BOYD, 1997a).

RODEN and SHIMIZU (1993) used depleted trace-element patterns in clinopyroxene from Colorado Plateau xenoliths to argue that these peridotites are equivalent to oceanic peridotites. However, the available Gnt-SCLM (Table 4) and whole rock data (Table 1) suggest that on average, the Colorado Plateau SCLM is distinct from oceanic peridotites.

Underplating of undepleted "asthenospheric" material at divergent margins or intraplate settings (*e.g.,* JOCHUM *et al.*, 1989) will not produce SCLM of any thickness, because on cooling the upper part of the section will be denser than the underlying asthenosphere and hence unstable (O'REILLY *et al.*, 1998; see below). STEIN and HOFMANN (1992, 1994) suggested that the SCLM is made up of fossilised plume heads, each a mixture of the plume source (already mildly depleted) and material entrained from the overlying mantle. The model is difficult to test by xenolith data, because different parts of such a plume might have very different characteristics, and available sample material is ambiguous. Xenoliths representing the mantle beneath the Deccan Traps are typical YETI lherzolites with average degrees of depletion of ≤5% (KARMALKAR, GRIFFIN and O'REILLY, in prep.) and are similar to the Zabargad peridotites and Arabian xenoliths, proposed as a fossil plume head by STEIN and HOFMANN (1992). Xenoliths and garnets from Malaita, believed to represent mantle beneath the plume-related Ontong-Java Plateau, also indicate low degrees of depletion (NIXON and BOYD, 1979; NEAL, 1988; Table 4). On the other hand, the Kerguelen xenoliths (Table 1) are spatially related to a very large plume (MATTIELLI *et al.*, 1996), and are highly depleted; these could represent either the interior parts of a plume, or remnant oceanic lithosphere. However, given the similarity between the Deccan and Malaita SCLM on the one hand, and the Zabargad and YETI SCLM on the other, the generation of most Phanerozoic SCLM by accumulation of plume heads appears to be consistent with the available data.

Causes of secular variation in SCLM composition

A plume-related model for generation of the SCLM is attractive because it involves a process that probably has been active in one form or another throughout Earth's history. It also provides a mechanism for producing secular change in the products, related to the secular cooling of Earth and to evolution in the composition of recycled material in plumes (CAMPBELL and GRIFFITHS, 1992; HOFMANN and WHITE, 1982). HERZBERG (1995) demonstrated that the compositions of high-degree melts (komatiites and picrites) become less ultramafic from Archean to present. Arguing that plumes represent a nearly constant 200°C temperature excess relative to the mantle adiabat, he interpreted the secular change in magma compositions to reflect an evolution toward progressively shallower depths of melting through time. Building on this argument, HERZBERG and ZHANG (1996) showed that the shape of the peridotite solidus requires the depth of melting to rise from 250 km to 200 km through the Archean (from 3.5 Ga to 2.7 Ga) and then to rise further to ca 80 km today. In this model, the degree of depletion of the residues also would decline through time, as progressively shallower melting at lower maximum temperatures produced lower average degrees of partial melting. The higher opx/olivine ratios of the Archean SCLM would be the result of melting at higher pressures (CANIL, 1992; Boyd, 1989, 1997a; WALTER, 1997).

However, models that rely on secular cooling alone are not completely satisfactory, since they offer no obvious explanation for the change in mantle processes near the Archean/Proterozoic boundary, nor for the apparently episodic generation of komatiites and continental crust in general. The MOMO (mantle overturns and major orogenies) model of STEIN and HOFMANN (1994) proposes an alternation through Earth's history between periods of two-layer convection and periods of whole-mantle convection, providing episodic magmatism and tectonism. If this model is combined with the effects of secular cooling of the mantle, so that each successive overturn resulted in plumes that produced less melt at shallower levels, it can explain the post-Archean evolution of lithospheric composition that we have described here.

DAVIES (1995) has proposed a model for Earth's thermal and dynamic evolution that offers a qualitative explanation for the evolution of subcontinental mantle documented here. This model is based on the secular cooling of a two-layered mantle. In Archean time, the upper mantle cools rapidly through heat loss at the surface, while the lower mantle warms due to heating from the core, and inefficient heat transfer across the boundary between the two layers. Over time, this divergence of temperatures leads to periodic massive overturn, bringing hot lower mantle rapidly to upper-mantle depths; this overturn could induce high-degree melting at relatively great depth as the rising material oversteps the dry peridotite

solidus. These processes might be responsible for the opx-rich, highly depleted residues (or cumulates) that characterise Archean mantle. The overturns become less frequent as the Earth cools, and the maximum temperature reached by the upper mantle becomes lower with each cycle. This model provides for a "catastrophic" regime of mantle (and crust) formation within the Archean, the disappearance of this regime near the Archean/Proterozoic boundary, and a gradual evolution in process through the Proterozoic and into the Phanerozoic, as required by the data presented here (GRIFFIN *et al.* 1998a, their Fig. 14).

Geophysical and geodynamic consequences

Table 5 shows estimates of modal composition, density and seismic velocities for the "best estimate" compositions of Archon, Proton and Tecton SCLM. Values also are given for a model asthenosphere of PUM composition. Modes were calculated using mean compositions for xenolith minerals from each age group; densities were derived from the modes using data on end-member mineral components (SMYTH and MCCORMICK, 1995), and extrapolated to a range of temperatures using the thermal expansion coefficients of FEI (1995). Seismic velocities (V_p and V_s) then were calculated using mean mineral compositions and end-member data compiled by ANDERSON (1989), modified according to Anderson and Isaak (1995). This procedure is regarded as superior to our earlier estimates, which used the algorithms of SIMMONS (1964) and ANDERSON and SAMMIS (1970) (see O'REILLY *et al.* (1990) for discussion). The calculated densities are most sensitive to mg# and olivine content, and least sensitive to gnt and cpx composition. Small contents of gnt and cpx do not significantly influence density, and there thus is little difference in density between Archean lherzolites and harzburgites.

The calculated mean density of Archon SCLM (Table 5) agrees well with BOYD and MCALLISTER'S (1976) calculated density for a strongly depleted Archean garnet lherzolite (PHN1569; d = 3.30 ±.02 g/cm^3). Their estimated density (3.39 ± .02 gm/cm^3) for high-T sheared peridotite PHN1611, a sample especially rich in gnt and cpx, is higher than our value for the average Archean high-T lherzolite. On average, Archean lherzolites and harzburgites are ≈0.05 g/cm^3 (1.5%) less dense than Phanerozoic lherzolite at any T. Despite its higher density, Phanerozoic mantle has a V_p ≈0.5% lower than that of Archean mantle because of the inverse relationship between density and V_p in olivine and orthopyroxene. The difference in V_s is larger (≈1.2%), and similar to that calculated by SOBOLEV *et al.* (1995).

GUDMUNDSSON and SAMBRIDGE (1998) analysed the V_p and V_s variation with depth beneath different types of tectonic provinces; they found differences of ≈3.5% in V_p and ≈4% in V_s (at 100 km depth) between ancient (>1.7 Ga) and young (<0.25 Ga) continental regions. SU *et al.* (1994) show a total range of ca 5% in V_s worldwide at similar depths. The data in Table 5 suggest that compositional differences between Archon and Tecton SCLM can account for ≈15% of the spread in V_p and 30% of the spread in V_s. The remainder probably reflects differences in the average geotherm between cratonic regions and mobile belts (cf JORDAN, 1988). Using typical geotherms for Archon, Proton and Tecton areas, we have calculated V_s and V_p at 50 km (where Tecton mantle will be in spinel peridotite facies) and 100 km (where all regions will be in garnet peridotite facies); at each depth the range in V_p and V_s is 4–5%, close to the observed values.

The differences in density between SCLM of different age have important tectonic consequences. Many analyses of lithosphere composition and dynamics regard even old SCLM as "cold and dense", and argue that such lithosphere can delaminate and founder, providing a mechanism for recycling SCLM through the deep mantle (*e.g.*, MCKENZIE and O'NIONS, 1983; HOUSEMAN and MOLNAR, 1997; HOFMANN, 1997). However, the highly depleted Archon SCLM is quite buoyant relative to "asthenosphere", even when significantly cooler (GRIFFIN *et al.*, 1998a, their Fig. 15) and hence can support a root of ≥200 km thickness without achieving negative buoyancy (O'REILLY *et al.*, 1998). Proton lithosphere, which is somewhat denser, still can support a root ≥150 km thick, as seen in many sections worldwide (O'REILLY *et al.*, 1998). However, the low degree of depletion in Tecton SCLM, and especially in the more fertile varieties, means that with cooling, it can become negatively buoyant relative to asthenosphere and thus cannot sustain a root. Similarly, the conversion of Archon or Proton SCLM to more "asthenospheric" compositions by high-T melt-related metasomatism (see below) will reduce the buoyancy of the lowest part of continental keels.

These data make it clear why the thickest SCLM ("continental roots" or "keels"), as observed in seismic tomography, is found beneath some Archean and Early-Middle Proterozoic cratons (POLET and ANDERSON, 1995): only in the early part of Earth history did SCLM-forming processes produce large volumes of material with the low density required to make these thick roots. As discussed above, these roots apparently have been coupled to the overlying cratonic crust since their formation. The absence of such a root beneath an Archon is unusual and implies its

removal, despite its refractory and buoyant nature. EGGLER *et al.* (1988) have shown that the Archean root was removed from beneath the Colorado-Wyoming craton in Cenozoic time, and suggested that it was displaced by the Laramide collision. Another possible mechanism is rifting, accompanied by mechanical and chemical mixing of the original root with younger, denser material, as appears to have occurred in eastern China during Tertiary time (GRIFFIN *et al.*, 1998b; YUAN, 1996).

If, as suggested above, the TILE xenolith suite and the European orogenic massifs represent Proterozoic SCLM, this SCLM was formed beneath the juvenile Proterozoic crust of Europe, and has survived several episodes of Phanerozoic orogenic reworking. More fertile, and probably younger mantle, appears to be present only at greater depths, or in areas of more pronounced extension, as in eastern Europe. These observations suggest that crustal reworking in compressional tectonic episodes generally is not be sufficient to remove older, depleted SCLM, and that formation of new SCLM requires extensional processes, and/or the formation of juvenile crust (*e.g.*, island arc environments).

The stresses involved in plate tectonics contribute directly to the foundering of relatively dense SCLM (HOUSEMAN and MOLNAR, 1996). It therefore seems likely that only the most buoyant material can survive as SCLM over geologic time, and that the evolution described here records only the most depleted material incorporated into the SCLM at each stage of Earth history. Less-depleted material, corresponding for example to modern abyssal peridotites, may have been produced in Archean time, but it would be difficult to preserve. Conversely, the rarity of highly depleted Archon-type material in the Proterozoic, and especially Phanerozoic, SCLM suggests that such material was not being added to SCLM during those periods. It should be noted that "metasomatism" (a favourite *deus ex machina* of mantle petrologists) will not contribute to preservation of less-depleted material; many styles of metasomatism involve introduction of Fe, Ca, Al and other elements that will increase, rather than decrease, density.

Residual peridotites with a high degree of depletion are being produced in some modern oceanic and active-margin environments (Table 1), yet little of this material is identifiable in xenolith suites from young SCLM. If most young SCLM sampled in this way is generated in extensional environments (JOCHUM *et al.*, 1989) or by accumulation of plume heads in intraplate environments (STEIN and HOFMANN, 1994), then any accreted oceanic material may simply be destroyed in this process. This would leave us with a biased record of the processes that build up the SCLM under new crust as it forms, but perhaps a more realistic picture of the generation of stable SCLM over the longer term. It also is possible that extensive metasomatism of the mantle wedge above subduction zones ultimately increases the density of the depleted mantle to the point that it cannot survive as SCLM.

High-T sheared lherzolites and the "asthenosphere"

Many kimberlites and some intraplate basalts contain a group of lherzolite xenoliths with high (≥1200 °C) equilibration temperatures and a variety of strain-related microstructures, ranging from mildly foliated to mylonitic (HARTE, 1977). These xenoliths typically have less depleted major-element compositions than the more common lower-temperature xenoliths with granular microstructures, which have provided the Archon data used in this paper. They also have high contents of garnet and clinopyroxene (BOYD and MERTZMAN, 1989), and extreme examples such as PHN1611 (SMITH and BOYD, 1987; SMITH *et al.*, 1993) approach "pyrolite" composition. This enriched major-element composition has led many workers regard the sheared high-T lherzolites as samples of asthenospheric material. Others (KESSON and RINGWOOD, 1989) have suggested they represent deformed and metasomatised oceanic peridotites, subducted and accreted on the bottom of lithospheric keels.

However, Archean Re-Os depletion ages (PEARSON *et al.*, 1995) indicate that these xenoliths are in fact fragments of Archean lithosphere. Zoned garnets (SMITH and BOYD, 1987; GRIFFIN *et al.*, 1989a; SMITH *et al.*, 1991, 1993) in these xenoliths have cores with the depleted compositions typical of Archon lithospheric garnets, overgrown by metasomatic rims that comprise up to 50% of the garnet. Diffusion modelling of the zoning profiles in these garnets indicates that the overgrowths formed very shortly (10–1000 years) before the magmatic event that brought the xenoliths to the surface. This is consistent with microstructural analysis (MERCIER and NICOLAS, 1975) that requires the strain (shearing) to have been proceeding at the time the xenoliths were entrained. These xenoliths therefore represent neither asthenosphere nor young subducted oceanic lithosphere; they are fragments of the ancient lithospheric keel, strongly metasomatised by the recent infiltration of asthenosphere-related melts (EHRENBERG, 1979; HARTE, 1983; SMITH and BOYD, 1987; SMITH *et al.*, 1993).

The importance of these xenoliths lies in the evidence they provide that the interaction between as-

thenosphere-derived melts and the base of the SCLM can change the composition, and hence the density (Table 5), of the lower SCLM to the point where it no longer is buoyant relative to the asthenosphere. This process may be important in the thinning and removal of older SCLM, especially in pre-rift stages.

CONCLUSIONS

1. Data from xenoliths, garnet concentrates and peridotite massifs demonstrate secular and episodic evolution in the composition of subcontinental lithospheric mantle (SCLM), related to the last major tectonothermal event in the overlying crust. Subcalcic (cpx-free) garnet harzburgites are restricted to Archean mantle, and the dominant lherzolites become progressively less depleted (in terms of major-element composition) from Archean through Proterozoic to Phanerozoic time.

2. Archean SCLM was derived by high-degree melting at depths >150 km, during which no Cr-Al phase was present in the residue. Observed compositional variations may reflect both sorting of olivine and high-T opx, and variable degrees of melt reaction, leading to more olivine-rich compositions.

3. Peridotites from convergent-margin settings and oceanic basins, as observed in ophiolites, abyssal peridotites and rare xenolith suites, generally have strongly depleted compositions, and do not appear to make up large parts of Phanerozoic SCLM. This observation suggests that accretion of subducted oceanic mantle probably is not the major process involved in the production of stable SCLM.

4. Comparison of xenolith-derived and garnet-derived mantle compositions from Tectons and modern environments favours an origin of most SCLM by accumulation of material from rising plumes (s.l.), largely in intraplate settings. Generation of SCLM in Phanerozoic extensional environments typically involves <10% partial melting, with a Cr-Al phase present on the liquidus. Proterozoic SCLM probably was generated by similar processes, but with higher average degrees of melting and possibly at greater depths. Such models can relate the secular evolution of SCLM composition to the secular cooling of Earth.

5. The correlation between crustal age and SCLM composition implies quasi-contemporaneous formation of crustal volumes and the underlying SCLM, and continued coupling between them for timespans measured in aeons. Archean SCLM is heterogeneous, in degree of depletion and stratigraphic distribution of rock types, on a terrane scale, suggesting that relatively small bodies of crust + SCLM were able to survive continental drift and accretion into cratons.

6. The density of mean Archean SCLM is ca 1.5% less than of mean Phanerozoic SCLM, which is only 0.6% less dense than pyrolitic material at the same temperature; Proterozoic SCLM is intermediate in density. These density differences explain the survival of thick (≥200 km) Archean lithosphere and the lack of lithospheric roots beneath Phanerozoic areas. Compositional differences also strongly affect seismic velocities; continental roots imaged beneath cratons by seismic tomography reflect compositional differences, reinforced by differences in the mean geotherm between Archean and younger areas.

7. The depleted, refractory Archean SCLM is buoyant relative to asthenosphere even when "cold", and cannot be "delaminated" by gravitational forces alone. The same is true, to a somewhat lesser degree, of Proterozoic SCLM. This situation greatly limits the potential for "recycling" of ancient SCLM, invoked by some isotopic models. However, episodes of continental rifting may mix Archean SCLM with younger, more fertile (and hence denser) material, which on cooling might eventually be delaminated; this could provide a mechanism for recycling.

Acknowledgments—We are grateful to Olivier Alard, Joe Boyd, Tony Carswell, Michel Gregoire, Dmitri Ionov, Yaoling Niu, Doug Smith and Xisheng Xu for providing unpublished data and data compilations, and giving us permission to use them. Olivier Alard, Eloise Beyer, Will Powell and Esme van Achterbergh helped enormously with compilation and organisation of the xenolith database. The ideas expressed in this paper have benefited greatly from discussions with Joe Boyd, Olivier Alard, Buddy Doyle, Oliver Gaul, Dmitri Ionov, Lynton Jaques, Kevin Kivi, Marc Norman, Norm Pearson, Ken Tainton, Bruce Wyatt and Ming Zhang – although they may not agree with everything. The final MS was improved through thoughtful and constructive reviews from Ben Harte, Bjørn Mysen and Doug Smith. This work has been supported by Macquarie University Collaborative Research Grants and Australian Research Council grants to WLG and SYOR. This is publication no. 132 from the ARC National Key Centre for Geochemical Evolution and Metallogeny of Continents (GEMOC).

REFERENCES

ALARD O., DAUTRIA J. M., and BODINIER J. -L. (1996) Nature and metasomatic processes of the lithospheric mantle on either part of Sillon Houiller (French Massif Central). *C.R. Acad. Sci. Paris* **323,** 763–770.

ALLEGRE C. J., POIRIER J. -P., HUMLER E., and HOFMANN A. W. (1995) The chemical composition of the earth. *Earth. Planet. Sci. Lett.* **134,** 515–526.

ANDERSON D. L. (1989) *Theory of the Earth.* Blackwell Scientific Publications, Boston.

ANDERSON D. L. (1995) Lithosphere, asthenosphere and perisphere. *Rev. Geophysics* **31,** 125–149.

ANDERSON D. L. and SAMMIS C. (1970) Partial melting in the upper mantle. *Phys. Earth Planet. Interiors* **3,** 41–50.

ANDERSON O. and ISAAK D. G. (1995) Elastic constants of mantle minerals at high temperatures. In *Mineral physics and crystallography: a handbook of physical constants*

(ed. T. J. AHRENS). pp. 64–97. Amer. Geophys. Union, Washington.

AOKI K. I. and SHIBA I. (1973) Pyroxenes from lherzolite inclusions of Itinome-gata, Japan. *Lithos* **6,** 41–51.

AOKI K. I. (1981) Major element geochemistry of chromian spinel peridotite xenoliths in the Green Knobs Kimberlite, New Mexico. *The Science Reports of the Tohoku University Sendai, Japan* **3rd Series V**

AUMENTO F. and LOUBAT H. (1971) The Mid-Atlantic Ridge near 45°N. XVI. Serpentinized ultramafic intrusions. *Can. Jour. Earth Sci.* **8,** 631.

BASALTIC VOLCANISM STUDY PROJECT (1981) *Basaltic Volcanism on the Terrestrial Planets.* Pergamon.

BECKER H. (1996) Geochemistry of garnet peridotite massifs from lower Austria and the composition of deep lithosphere beneath a Palaeozoic convergent plate margin. *Chem. Geol.* **134,** 49–65.

BERGER E. (1964) Le volcanisme des Causses lozeriens. D.E.S. Thesis, Paris-Sud Orsay, 74p.

BERGER T. (1981) Enclaves ultramafiques, megacristaux et leurs basaltes hotes en contexte oceanique (Pacifique Sud) et continental (Massif Central, Francais). PhD thesis, Paris-Sud, Orsay.

BICKLE M. J., FORD C. E., and NISBET E. G. (1977) The petrogenesis of peridotitic komatiites: evidence from high-pressure melting experiments. *Earth Planet. Sci. Lett.* **37,** 97–106.

BLOOMER S. H. (1983) Distribution and origin of igneous rocks from the landward slopes of the Mariana trench: implications for its structure and evolution. *J. Geophys. Res.* **88,** 7411–7428.

BODINIER J. L., DUPUY C. and DOSTAL J. (1988) Geochemistry and petrogenesis of Eastern Pyrenean peridotites. *Geochim. Cosmochin. Acta* **52,** 2893–2907.

BODINIER J. L. (1988) Geochemistry and petrogenesis of the Lanzo peridotite body, western Alps. *Tectonophysics* **149,** 67–88.

BONATTI E. and MICHAEL P. J. (1989) Mantle peridotites from continental rifts to ocean basins to subduction zones. *Earth Planet. Sci. Lett.* **91,** 297–311.

BONATTI E., HAMLYN P., and OTTONELLO G. (1981) Upper mantle beneath a young oceanic rift: Peridotites from the island of Zabargad (Red Sea). *Geology* **9,** 474–479.

BONATTI E., OTTONELLO G., and HAMLYN P. R. (1986) Peridotites from the island of Zabargad (St. John), Red Sea: petrology and geochemistry. *J. Geophys. Res.* **91,** 599–631.

BOUDIER F. and AHRENS T. J. (1985) Harzburgite and lherzolite subtypes in ophiolitic and ocean environments. *Earth Planet. Sci. Lett.* **76,** 84–92.

BOYD F. R. (1989) Composition and distinction between oceanic and cratonic lithosphere. *Earth Planet. Sci. Lett.* **96,** 15–26.

BOYD F. R. (1997a) Origin of peridotite xenoliths: major element considerations. In *High pressure and high temperature research on lithosphere and mantle materials* (eds. G. RANALLI, F. RICCI LUCCHI, C. A. RICCI, and T. TROMMSDORFF). Univ. of Siena.

BOYD F. R. (1997b) Correlation of orthopyroxene abundance with the Ni content of coexisting olivine in cratonic peridotites. AGU 1997 Fall meeting, Abst.

BOYD F. R. and MCALLISTER R. H. (1976) Densities of fertile and sterile garnet peridotites. *Geophys. Res. Lett.* **3,** 509–512.

BOYD F. R. and MERTZMAN S. A. (1987) Composition and structure of the Kaapvaal lithosphere, southern Africa. In *Magmatic processes: physicochemical principles* (ed. B. O. MYSEN). *Geochem. Soc. Spec. Publ.* **1,** 13–24.

BOYD F. R., PEARSON D. G., NIXON P. H., and MERTZMAN S. A. (1993) Low-calcium harzburgites from southern Africa: their relations to craton structure and diamond crystallization. *Contrib. Mineral. Petrol.* **113,** 352–366.

BOYD F. R., POKHILENKO N. P., PEARSON D. G., MERTZMAN S. A., SOBOLEV N. V., AND FINGER L. W. (1997) Composition of the Siberian cratonic mantle: evidence from Udachnaya peridotite xenoliths. *Contrib. Mineral. Petrol.* **128,** 228–246.

BROUSSE R. (1961) Minéralogie et petrographie des roches volcaniques des massifs du Mont Dore (Auvergne). *Bull. Soc. Fr. Min. Crist.* **84,** 131–259.

BROUSSE R. (1968) La place des ultra-basites en France. *Geologische Rundschau* **57,** 621–655.

BURWELL A. D. M. (1975) Rb-Sr isotope geochemistry of lherzolites and their constituent minerals from Victoria, Australia. *Earth Planet. Sci. Lett.* **28,** 69–78.

CAO R. L. and ZHU S. H. (1983) Correlation of mantle xenolith occurrences with Earth's internal zoning and structure in eastern China. *Acta Geophysica Sinica* **26,** 158–167(in Chinese).

CAMPBELL I. H. and GRIFFITHS R. W. (1992) The changing nature of mantle hotspots through time: implications for the chemical evolution of the mantle. *J. Geol.* **92,** 497–523.

CANIL D. (1991) Experimental evidence for the exsolution of cratonic peridotite from high-temperature harzburgite. *Earth Planet. Sci. Lett.* **106,** 64–72.

CANIL D. (1992) Orthopyroxene stability along the peridotite solidus and the origin of cratonic lithosphere beneath southern Africa. *Earth Planet. Sci. Lett.* **111,** 83–95.

CANIL D. and WEI K. (1992) Constraints on the origin of mantle-derived low Ca garnets. *Contrib. Mineral. Petrol.* **109,** 421–430.

CARSWELL D. A. (1968) Possible primary upper mantle peridotite in Norwegian Basal Gneisses. *Lithos* **1,** 322–355.

CARSWELL D. A. and DAWSON J. B. (1970) Garnet peridotite xenoliths in South African Kimberlite Pipes and their petrogenesis. *Contrib. Mineral. Petrol.* **25,** 163–184.

CARSWELL D. A., CLARKE D. B., and MITCHELL R. H. (1979) The petrology and geochemistry of ultramafic nodules from Pipe 200, northern Lesotho. In *The mantle sample: Inclusions in kimberlites and other volcanics* (eds. F. R. BOYD and H. O. A. MEYER). pp. 127–145. American Geophysical Union, Washington D.C.

CARSWELL D. A., GRIFFIN W. L., and KRESTEN P. (1984) Peridotite nodules from the Ngopetseou and Lipelaneng kimberlites, Lesotho: A crustal or mantle origin - Appendix. *Ann. Soc. Univ. Clermont-Fd,* **II 74,** 167–178.

CAUSSE, C. R. (1965) Les appareils eruptifs de la region de Millau (France). D.E.S. Thesis, Paris-Sud, Orsay.

CHEN C. -Y., FREY F. A., and SONG Y. (1989) Evolution of the upper mantle beneath southeast Australia: geochemical evidence from peridotite xenoliths in the Mount Leura basanite. *Earth Planet Sci. Lett.* **93,** 195–209.

CLAGUE D. A. (1987) Hawaiian xenolith populations, magma supply rates, and development of magma chambers. *Bull Volcanol.* **49,** 577–587.

COHEN A. S., BURNHAM O. M., ROGERS N. W., and MARTYN K. (1996) Re-Os systematics of peridotite xenoliths from Dreiser Weiher and Gees, Eifel, Germany, *Abst. 6th Goldschmidt Conf.,* 116.

COMIN-CHIARAMONTE P., DEMARCHI G., GIRARDI V. A. V., PRINCIVALLE F., and SINIGOI S. (1986). Evidence of man-

tle metasomatism and heterogeneity from peridotite inclusions of northeastern Brazil and Paraguay. *Earth Planet. Sci. Lett.* **77,** 203–217.

CONQUERE F. (1970) La Lherzolite a amphibole du gisement de Caussou (Ariege, France). *Contrib. Mineral. Petrol.* **30,** 296–313.

COX K. G., GURNEY J. J., and HARTE B. (1973). Xenoliths from the Matsoku Pipe. In *Lesotho Kimberlites* (ed. P. H. NIXON). pp. 76-92. Lesotho National Development Corporation.

COX K. G., SMITH M. R., and BESWETHERICK S. (1987) Textural studies of garnet lherzolites: evidence of exsolution origin from high-temperature harzburgites. In *Mantle Xenoliths* (ed. P. H. NIXON). pp 537–550. Wiley.

DANCHIN R. V. (1977) Mineral and bulk chemistry of garnet lherzolite and garnet harzburgite xenoliths from the Premier Mine, South Africa. In *The mantle sample: Inclusions in kimberlites and other volcanics* (eds. F. R. BOYD and H. O. A. MEYER). pp. 104–127. American Geophysical Union, Washington D.C.

DAUTRIA J. M. and GIROD M. (1986) Les enclaves de lherzolite a spinelle et plagioclase du volcan DeDibi (Adamoua, Camerou): des temoins d'un manteau superieur anormal. *Bull. Mineral* **109,** 275–288.

DAVIES G. F. (1995) Punctuated tectonic evolution of the earth. *Earth Planet. Sci. Lett.* **136,** 363–379.

DICK H. J. B., BULLEN T., and BRYAN W. B. (1984) Mineralogic variability of the uppermost mantle along mid-ocean ridges. *Earth Planet. Sci. Lett.* **69,** 88–106.

DOWNES H. and DUPUY C. (1987) Textural, isotopic and REE variations in spinel peridotite xenoliths, Massif Central, France. *Earth Planet. Sci. Lett.* **82,** 121–135.

DOWNES H., EMBEY-ISZTIN A., and THIRLWALL M. F. (1992) Petrology and geochemistry of spinel peridotite xenoliths from the Western Pannonian Basin (Hungary): evidence for an association between enrichment and texture in the upper mantle. *Contrib. Mineral . Petrol.* **109,** 340–354.

DUPUY C., DOSTAL J., and BOIVIN P. A. (1986) Geochemistry of ultramafic xenoliths and their host alkali basalts from Tallante, southern Spain. *Mineral. Mag.* **59,** 231–9.

DUPUY C., DOSTA J., and BODINIER J. L. (1987) Geochemistry of spinel peridotite inclusions in basalts from Sardinia. *Mineral. Mag.* **51,** 561–568.

EHRENBERG S. M. (1979) Garnetiferous ultramafic inclusions in minette from the Navajo volcanic field. In *The mantle sample: Inclusions in kimberlites and other volcanics* (eds. F. R. BOYD and H. O. A. MEYER). pp. 330–344. Amer. Geophys. Union, Washington D.C.

EGGLER D. H., MEEN J. K., WELT R., DUDAS F. O., FURLONG K. P., MCCALLUM M. E., and CARLSON R. W. (1988). Tectonomagmatism of the Wyoming Province. *Colorado School of Mines Quarterly* **83,** 25–40.

ERNST W. G. (1978) Petrochemical study of lherzolitic rocks from the Western Alps. *J. Petrol.* **19,** 341–392.

ERNST W. G. and PICCARDO G. B. (1979) Petrogenesis of some Ligurian peridotites-I. Mineral and bulk-rock chemistry. *Geochim. Cosmochim. Acta* **43,** 219–237.

FABRIES J., LORAND J. -P., BODINIER J. -L., and DUPUY C. (1991) Evolution of the upper mantle beneath the Pyrenees: evidence from orogenic spinel peridotite massifs. *J. Petrol.* Special Lherzolite Volume, 55–76.

FAN Q. C. and HOOPER P. R. (1989) The mineral chemistry of ultramafic xenoliths of eastern China: Implications for upper mantle composition and the paleogeotherm. *J. Petrol.* **30,** 1117–1158.

FEI Y. (1995) Thermal expansion. In *Mineral physics and crystallography: a handbook of physical constants* (ed. T. J. AHRENS). pp. 29–44. Amer. Geophys. Union, Washington, D.C.

FEIGENSON M. D. (1986) Constraints on the origin of Hawaiian lavas. *J. Geophys. Res.* **91,** 9383–9393.

FOUNTAIN D. M. and SALISBURY M. H. (1981) Exposed cross-sections through the continental crust: implications for crustal structure, petrology, and evolution. *Earth Planet. Sci. Lett.* **56,** 263–277.

FREY F. A. and GREEN D. H. (1974) The mineralogy, geochemistry and origin of lherzolite inclusions in Victorian basanites. *Geochim. Cosmochim. Acta* **38,** 1023–1059.

FREY F. A. and PRINZ M. (1978) Ultramafic inclusions from San Carlos, Arizona: petrologic and geochemical data bearing on their petrogenesis. *Earth Planet. Sci. Lett.* **38,** 129–176.

FREY F. A., SUEN C. J., and STOCKMAN H. W. (1985) The Ronda high temperature peridotite: geochemistry and petrogenesis. *Geochim. Cosmochim. Acta* **49,** 2469–2491.

FREY F. A., CHEN C. -Y., and SONG Y. (1989) Evolution of the upper mantle beneath southeast Australia: geochemical evidence from peridotite xenoliths in Mount Leura basanite. *Earth Planet. Sci. Lett.* **93,** 195–209.

GRIFFIN W. L., SMITH D., BOYD F. R., COUSENS D. R., RYAN C. G., SIE S. H., and SUTER G. F. (1989a) Trace element zoning in garnets from sheared mantle xenoliths. *Geochim. Cosmochim. Acta* **53,** 561–567.

GRIFFIN W. L., RYAN C. G., COUSENS D. C., SIE S. H., and SUTER G. F. (1989b) Ni in Cr-pyrope garnets: a new geothermometer. *Contrib. Mineral. Petrol.* **103,** 199–202.

GRIFFIN W. L. and RYAN C. G. (1995) Trace elements in indicator minerals: area selection and target evaluation in diamond exploration. *J. Geochem. Explor.* **53,** 311–337.

GRIFFIN W. L., RYAN C. G., O'REILLY S. Y., and GURNEY J. J. (1995) Lithosphere evolution beneath the Kaapvaal craton: 200-90 Ma. *Abst. 6th Int. Kimberlite Conf.,* 203–204.

GRIFFIN W. L., KAMINSKY F. V., RYAN C. G, O'REILLY S. Y., WIN T. T., and ILUPIN I. P. (1996) Thermal state and composition of the lithospheric mantle beneath the Daldyn kimberlite field, Yakutia. *Tectonophysics* **262,**19–33.

GRIFFIN W. L., O'REILLY S. Y., RYAN C. G., GAUL O., and IONOV D. A. (1998a) Secular variation in the composition of subcontinental lithospheric mantle: Geophysical and geodynamic implications. In *Structure & Evolution of the Australian Continent* (eds. J. BRAUN, J. C. DOOLEY, B. R. GOLEBY, R. D. VAN DER HILST and C. T. KLOOTWIJK). pp. 1–26. *Geodynamics Vol. 26,* Amer. Geopyhys. Union, Washington D.C.

GRIFFIN W. L., ZHANG A., O'REILLY S. Y., and RYAN C. G. (1998b) Phanerozoic evolution of the lithosphere beneath the Sino-Korean Craton. In *Mantle dynamics and plate interactions in east Asia* (eds. M. FLOWER, S.L CHUNG, C.H.LO and T. Y. LEE) pp. 107–126. *Geodynamics vol. 27,* Amer. Geophys. Union, Washington D.C.

GRIFFIN W. L., FISHER N. I., FRIEDMAN J., RYAN C. G., and O'REILLY S. Y. (1998c) Cr-pyrope garnets in the lithospheric mantle. I. Compositional systematics and relationships to tectonic setting. *J. Petrol.* 40 (in press).

GRIFFIN W. L., RYAN C. G., KAMINSKY F. V., O'REILLY S. Y., NATAPOV L. M., WIN T. T., KINNY P. D., and ILUPIN I. P. (1998d) The Siberian Lithosphere Traverse: Mantle terranes and the assembly of the Siberian Craton. *Tectonophysics* (in press)

GUDMUNDSSON O. and SAMBRIDGE M. (1998) A regionalized upper mantle (RUM) seismic model. *J. Geophys. Res.* **103,** 7121–7136.

GURNEY J. J. (1984) A correlation between garnets and diamonds. In *Kimberlite occurrence and origins: a basis for conceptual models in exploration* (eds. J. E. GLOVER and P. G. HARRIS). Geol. Dept. and Univ. Extension, Univ. Western Australia, Publ. No. 8, 143–166.

GURNEY J. J. and ZWEISTRA P. (1995) The interpretation of major-element compositions of mantle minerals in diamond exploration. *J. Geochem. Explor.* **53,** 293–310.

HANDLER M. R., BENNETT C. V., and ESAT T. M. (1997) The persistence of off-cratonic lithospheric mantle: Os isotopic systematics of variably metasomatised southeast Australian xenoliths. *Earth Planet. Sci. Lett.* **151,** 61–76.

HARTE B. (1977) Rock nomenclature with particular relation to deformation and recrystallisation textures in olivine-bearing xenoliths. *J. Geology* **85,** 279–288.

HARTE B. (1983) Mantle peridotites and processes – the kimberlite sample. In *Continental basalts and mantle xenoliths* (eds. C. J. HAWKESWORTH and M. J. NORRY). pp. 46–91. Shiva Publ. Co., Cheshire.

HARTMANN G. and WEDEPHOL H. K. (1990) Metasomatically altered peridotite xenoliths from the Hessian Depression (Northwest Germany). *Geochim. Cosmochim. Acta* **54,** 71–86.

HEBERT R., BIDEAU D., and HEKINIAN R. (1983) Ultramafic and mafic rocks from the Garrett Transform Fault near 13°30'S on the East Pacific Rise: igneous petrology. *Earth Planet. Sci. Lett.* **65,** 107–125.

HEINRICH W. and BESCH T. (1992) Thermal history of the upper mantle beneath a young back-arc extensional zone: ultramafic xenoliths from San Luis Potosí, Central Mexico. *Contrib. Mineral. Petrol.* **111,** 126–142.

HERZBERG C. (1990) Origin of mantle peridotite: constraints from melting experiments to 16.5 GPa. *J. Geophys. Res.* **95,** 15779–15803.

HERZBERG C. (1995) Generation of plume magmas through time: an experimental perspective. *Chem. Geol.* **126,** 1–16.

HERZBERG C. and ZHANG J. (1996) Melting experiments on anhydrous peridotite KLB-1: Compositions of magmas in the upper mantle and transition zone. *J. Geophys. Res.* **101,** 8271–8295.

HOAL B. G., HOAL K. E. O., BOYD F. R., and PEARSON D. G. (1995) Age constraints on crustal and mantle lithosphere beneath the Gibeon kimberlite field, Namibia. *S. Afr. Tydskr. Geol.* **98,** 112–118.

HOERNLE K., ZHANG Y. -S., and GRAHAM D. (1995) Seismic and geochemical evidence for large-scale mantle upwelling beneath the eastern Atlantic an western and central Europe. *Nature* **374,** 34–39.

HOFMANN A. W. and WHITE W. M. (1982) Mantle plumes from ancient oceanic crust. *Earth Planet. Sci. Lett.* **57,** 421–436.

HOFMANN A. (1997) Mantle geochemistry: the message from oceanic volcanism. *Nature* **385,** 219–229.

HOUSEMAN G. A. and MOLNAR P. (1997) Gravitational (Rayleigh-Taylor) instability of a layer with non-linear viscosity and convective thinning of continental lithosphere. *Geophys. J. Internat.* **128,** 125–150.

HUTCHISON R., WILLIAMS C. T., and HENDERSON P. (1986) New varieties of mantle xenolith from the Massif Central, France. *Mineral. Mag.* **50,** 559–565.

IONOV D. A. and WOOD B. J. (1992) The oxidation state of subcontinental mantle: oxygen thermobarometry of mantle xenoliths from central Asia. *Contrib. Mineral. Petrol.* **111,** 179–193.

IONOV D. A., ASHCHEPKOV I. V., STOSCH H. -G., WITT-EICKSCHEN G., and SECK H. A. (1993) Garnet peridotite xenoliths from the Vitim volcanic field, Baikal region: the nature of the garnet-spinel transition zone in the continental mantle. *J. Petrol.* **34,** 1141–1175.

IONOV D. A. and HOFMANN A. W. (1995) Nb-Ta-rich mantle amphiboles and micas: Implications for subduction-related metasomatic trace element fractionations. *Earth. Planet. Sci. Lett.* **131,** 341–356.

JAGOUTZ E., PALME H., BADDENHAUSEN H., BLUM K., CENDALES M., DREIBUS G., SPETTEL B., LORENZ V., and WANKE H. (1979) The abundance of major, minor and trace elements in the earth's mantle as derived from primitive ultramafic nodules. *Proc. 10th Lunar Planet. Sci. Conf.* 2031–2050.

JAMTVEIT B., CARSWELL D. A., and MEARNS E. W. (1991) Chronology of the high-pressure metamorphism of Norwegian garnet peridotites/pyroxenites. *J. Metam. Geology* **9,** 125–139.

JANSE A. J. A. (1994) Is Clifford's Rule still valid? Affirmative examples from around the world. In *Diamonds: characterization, genesis and exploration* (eds. H. O. A. MEYER and O. LEONARDOS) pp. 215-235. CPRM Spec. Publ. **1A/93,** Dept. Nacional da Prod. Mineral., Brazilia.

JAQUES A. L. and CHAPPELL B. W. (1980) Petrology and trace element geochemistry of the Papuan Ultramafic Belt. *Contrib. Mineral. Petrol.* **75,** 55–70.

JAQUES A. L., CHAPPELL B. W., and TAYLOR S. R. (1983) Geochemistry of cumulus peridotites and gabbros from the Marum Ophiolite Complex, northern Papua New Guinea. *Contrib. Mineral. Petrol.* **82,** 154–164.

JAQUES A. L., HALL A. E., SHERATON J. D., SMITH C. B., SUN S. -S., DREW D. M., FOLUDOULIS C., and ELLINGSEN K. (1989). Composition of crystalline inclusions and C-isotopic composition of Argyle and Ellendale diamonds. *Geol. Soc. Aust. Spec. Publ.* **14,** 966–989.

JAQUES A.L., O'NEILL H. ST. C., SMITH C. B., MOON J., and CHAPPELL B. W. (1990) Diamondiferous peridotite xenoliths from the Argyle (AKl) lamproite pipe, Western Australia. *Contrib. Mineral. Petrol.* **104,** 255–276.

JOCHUM K. P., MCDONOUGH W. F., PALME H., and SPETTEL B. (1989) Compositional constraints on the continental lithospheric mantle from trace elements in spinel peridotite xenoliths. *Nature* **340,** 548–550.

JORDAN T. H. (1988) Structure and formation of the continental lithosphere. *J. Petrol.* Special Lithosphere Issue, 11–37.

KELEMEN P. B., DICK H. J. B., and QUICK J. E. (1992) Formation of harzburgite by pervasive melt/rock reaction in the upper mantle. *Nature* **358,** 635–641.

KELEMEN P. B. and HART S. R. (1996) Silica enrichment in the continental lithosphere via melt-rock reaction. *Abst. 6th Goldschmidt Conf.,* 308.

KELEMEN P. B. and BERNSTEIN S. (1997) SiO_2 addition to cratonic mantle via melt-rock reaction above subduction zones. Abst. 1997 AGU, Abst.

KESSON S. E. and RINGWOOD A. E. (1989) Slab-mantle interactions I. Sheared and refertilised garnet peridotite xenoliths - samples of Wadati-Benioff zones? *Chem. Geol.* **78,** 83–96.

KUDO A. M., BROOKINS D. G., and LAUGHLIN A. W. (1972) Sr isotopic disequilibrium in Lherzolites from the Puerco Necks, New Mexico. *Earth Planet. Sci. Lett.* **15,** 291–295.

KUNO H. and AOKI K. I. (1970) Chemistry of ultramafic

nodules and their bearing on the origin of basaltic magmas. *Phys. Earth Planet. Inter.* **3,** 273–301.

LAMBERT D. D., SHIREY S. B., and BERGMAN S. C. (1995) Proterozoic lithospheric mantle source for the Prairie Creek lamproites: Re-Os and Sm-Nd isotopic evidence. *Geology* **23,** 273–276.

LAUGHLIN A. W., BROOKINS D. G., KUDO A. M., and CAUSEY J. D. (1971) Chemistry and Sr isotopic investigations of ultramafic inclusions and basalts, Bandera Crater, New Mexico. *Geochim. Cosmochim. Acta* **35,** 107–113.

LENOIR X., DAUTRIA J. -M., and BODINIER J. -L. (1997) Les enclaves mantelliques protogranulaires du Forez: temoins de l'erosion lithospherique en bordure du panache du Massif Central. *C. R. Acad. Sci.,* Paris **325,** 235–241.

LIANG Y. and ELTHON D. (1990) Geochemistry and petrology of spinel lherzolite xenoliths from Xalapascode La Joya, San Luis Potosi, Mexico: partial melting and mantle metasomatism. *J. Geophys. Res.* **95 B10,** 15859–15877.

LIPPARD S. J., SHELTON A. W., and GASS I. G. (1986) The ophiolite of northern Oman. *Memoir Geol. Soc. London* **11,** 54–127.

LIU R. X. and FAN Q. C. (1990) Major and trace element geochemistry of ultramafic xenoliths in Eastern China. In *Essays on the upper mantle beneath China and geodynamics.* pp. 45–61 (Seismological Press, Beijing).

LONEY R. A., HIMMELBERG G. R., and COLEMAN R. G. (1971) Structure and petrology of the alpine-type peridotite at Burro Mountain, California, U.S.A. *J. Petrol.* **12,** 245–309.

LORAND J. -P. and ALARD O. (1998) Geochemistry of incompatible trace elements and platinum group elements of the sub-continental lithospheric mantle: a coupled study in some peridotite xenoliths from the Massif Central (France). *Chem. Geol.* (submitted)

MAALOE S. and AOKI K. (1977) The major element composition of the upper mantle estimated from the composition of lherzolites. *Contrib. Mineral. Petrol.* **63,** 161–173.

MCBRIDE J. S., LAMBERT D. D., GREIG A., and NICHOLLS I. A. (1996) Multistage evolution of Australian subcontinental mantle: Re-Os constraints from Victorian mantle xenoliths. *Geology* **24,** 631–634.

MCCARRON J. M. (1997) Mantle provinciality in eastern Australia. Unpubl. MSc. thesis, Macquarie University.

MCDONOUGH W. F. (1990) Constraints on the composition of the continental lithospheric mantle. *Earth Planet. Sci. Lett.* **101,** 1–18.

MCDONOUGH W. F. and SUN S. (1995) The composition of the Earth. *Chem. Geol.* **120,** 223–253.

MCGUIRE A. V. (1988a) The mantle beneath the Red Sea Margin: xenoliths from Western Saudi Arabia. *Tectonophysics* **150,** 101–119.

MCGUIRE A. V. (1988b) Petrology of mantle xenoliths from Harrat al Kishb: the mantle beneath western Saudi Arabia. *J. Petrol.* **2,** 73–92.

MCKENZIE D. and BICKLE M. J. (1988) The volume and composition of melt generated by extension of the lithosphere. *J. Petrol.* **29,** 625–679.

MCKENZIE D. and O'NIONS R. K. (1983) Mantle reservoirs and ocean island basalts. *Nature* **301,** 229–331.

MATTIELLI N., WEIS D., GREGOIRE M., MENNESSIER J. P., COTTIN Y. J., and GIRET A. (1996) Kerguelen basic and ultrabasic xenoliths: Evidence for long-lived Kerguelen hotspot activity. *Lithos* **37,** 261–280.

MAURY R. C., DEFANT M. J., and JORON J. L. (1992) Metasomatism of the sub-arc mantle inferred from trace elements in Philippine xenoliths. *Nature* **360,** 661–663.

MEISEL T., BIINO G. G., and NAGLER T. F. (1996a) Re-Os, Sm-Nd, and rare-earth element evidence for Proterozoic oceanic and possible subcontinental lithosphere in tectonized ultramafic lenses from the Swiss Alps. *Geochim. Cosmochim. Acta* **60,** 2583–2593.

MEISEL T., WALKER R. J., and MORGAN J. W. (1996b) The osmium isotopic composition of the Earth's primitive upper mantle. *Nature* **383,** 517–520.

MENZIES M. A. (1991) Oceanic Peridotites. In *Oceanic Basalts* (ed. P. A. FLOYD). pp. 363–385. Blackie.

MENZIES M. A. (1990) Archean, Proterozoic and Phanerozoic lithospheric mantle. In *Continental Mantle* (ed. M. A. MENZIES). Oxford Univ. Press.

MENZIES M. A. and DUPUY C. (1991) Orogenic Massifs: protolith, process and provenance. *J. Petrol.* Special Lherzolites Issue, 1–16.

MERCIER J. C. and NICOLAS A. (1975) Textures and fabrics of upper-mantle peridotites as illustrated by xenoliths from basalts. *J. Petrol.* **16,** 454–487.

MICHAEL P. J. and BONATTI E. (1985) Peridotite composition from the North Atlantic: regional and tectonic variations and implications for partial melting. *Earth Planet. Sci. Lett.* **73,** 91–104.

NEAL C. R. (1988) THE ORIGIN AND COMPOSITION OF METASOMATIC FLUIDS AND AMPHIBOLES BENEATH MALAITA, SOLOMON ISLANDS. *J. PETROL.* **29,** 149–179.

NIELSON J. E., BUDAHN J. R., UNRUH D. M., and WILSHIRE H. G. (1992) Actualistic models of mantle metasomatism documented in a composite xenolith from Dish Hill, California. *Geochim. Cosmochim. Acta* **57,** 105–121.

NIMZ G. J., CAMERON K. L., and NIEMEYER S. (1995) Formation of mantle lithosphere beneath northern Mexico: Chemical and Sr-Nd-Pb isotopic systematics of peridotite xenoliths from La Olivina. *J. Geophys. Res.* **100,** 4181–4196.

NIU Y. (1997) Mantle melting and melt extraction processes beneath ocean ridges: evidence from abyssal peridotites. *J. Petrol.* **38,** 1047–1074.

NIU Y. and HEKINAN R. (1997) Basaltic liquids and harzburgitic residues in the Garrett Transform: a case study at fast-spreading ridges. *Earth Planet. Sci. Lett.* **146,** 243–258.

NICOLAS A., BOUDIER F., and BOUCHEZ J. -L. (1980) Interpretation of peridotite structures from ophiolitic and oceanic environments. *Amer. J. Sci.* **280,** 192–210.

NIXON P. H. (1987) Kimberlitic xenoliths and their cratonic setting. In *Mantle Xenoliths* (ed. P. H. NIXON) pp. 215–239. Wiley.

NIXON P. H. and BOYD F. R. (1973) Petrogenesis of the granular and sheared ultrabasic nodule suite in kimberlite. In *Lesotho Kimberlites* (ed. P. H. NIXON), pp. 48–57. Lesotho National Development Corporation.

NIXON P. H. and BOYD F. R. (1979) Garnet-bearing lherzolites and discrete nodule suites from the Malaita alnoite, Solomon Islands, S.W. Pacific, and their bearing on oceanic composition and geotherm. In *The mantle sample: inclusions in kimberlites and other volcanics* (eds. F. R. BOYD and H. A. O. MEYER). pp. 400–422. Amer. Geophys. Union, Washington D.C.

NORMAN M. D. (1998) Melting and metasomatism in the continental lithosphere: laser ablation ICPMS analysis of minerals in spinel lherzolites from eastern Australia. *Contrib. Mineral. Petrol.* **130,** 240–255.

O'HARA M. J., SAUNDERS M. J., and MERCY E. L. P. (1975) Garnet peridotite, primary ultrabasic magma and eclogite: interpretation of upper mantle processes in kimberlite. *Phys. Chem. Earth* **9,** 571–604.

O'REILLY S. Y. and GRIFFIN W. L. (1987) Eastern Australia-

4000 km of mantle samples. In *Mantle xenoliths.* (ed. P. H. NIXON) pp. 267–280. Wiley.

O'REILLY S. Y. and GRIFFIN W. L. (1988) Mantle metasomatism beneath western Victoria, Australia, I: Metasomatic processes in Cr-diopside lherzolites. *Geochim. Cosmochim. Acta* **52,** 433–437.

O'REILLY S. Y., GRIFFIN W. L., and GAUL O. (1997) Paleogeothermal gradients in Australia: Key to 4-D lithosphere mapping. *AGSO J. Australian Geol. Geophys.* **17,** 63–72.

O'REILLY S. Y., JACKSON I., and BEZANT C. (1990) Seismic and thermal parameters of upper mantle rocks from eastern Australia: implications for seismic modelling. *Tectonophysics* **185,** 67–82.

O'REILLY S. Y., GRIFFIN W. L., and POUDJOM DJOMANI Y. (1998) Are lithospheres forever? *Ext. Abst. 7th Int. Kimberlite Conf.,* 646–648.

OTTONELLO G., JORON J. L., and PICCARDO G. B. (1984) Rare earth and 3rd transition element geochemistry of peridotitic rocks: II. Ligurian peridotites and associated basalts. *J. Petrol.* **25,** 373–393.

PARSONS T. and MCCARTHY J. (1995) The active southwest margin of the Colorado Plateau: uplift of mantle origin. *Geol. Soc. Amer. Bull.* **107,** 139–147.

PAUL D. K. (1971) Strontium isotope studies on ultramafic inclusions from Dreiser Weiher, Eifel, Germany. *Contrib. Mineral. Petrol.* **34,** 22–28.

PEARSON D. G., CARLSON R. W., SHIREY S. B., BOYD F. R., and NIXON P. H. (1995) The stabilisation of Archaean lithospheric mantle: a Re-Os isotope study of peridotite xenoliths from the Kaapvaal and Siberian Cratons. *Earth Planet. Sci. Lett.* **134,** 341–357.

PEARSON N. J., GRIFFIN W. L., DOYLE B. J., O'REILLY S. Y., VAN ACHTERBERGH E., and KIVI K. (1998) Xenoliths from kimberlite pipes of the Lac de Gras area, Slave Craton, Canada. *Proc. 7th Int. Kimberlite Conf.* (in press)

POLET J. and ANDERSON D. L. (1995) Depth extension of cratons as inferred from tomographic studies. *Geology* **23,** 205–208.

PRESS S., WITT G., SECK H. A., IONOV D., and KOVALENKO V. I. (1986) Spinel peridotite xenoliths from the Tariat Depression, Mongolia. I: Major element chemistry and mineralogy of a primitive mantle xenolith suite. *Geochim. Cosmochim. Acta* **50,** 2587–2599.

QI Q., BEARD B. L., JIN Y., and TAYLOR L. A. (1994) Petrology and geochemistry of Al-augite and Cr-diopside group mantle xenoliths from Tahiti, Society Islands. *Intern. Geol. Rev.* **36,** 152–178.

QI Q., TAYLOR L. A., and ZHOU X. (1995) Petrology and geochemistry of mantle peridotite xenoliths from SE China. *J. Petrol.* **36,** 55–79.

REISBERG L. and LORAND J. -P. (1995) Longevity of subcontinental mantle lithosphere from osmium isotope systematics in orogenic peridotite massifs. *Nature* **376,** 159–162.

RICHARDSON S. H., GURNEY J. J., ERLANK A. J., and HARRIS J. W. (1984) Origin of diamonds in old enriched lithosphere. *Nature* **310,** 198–202.

RITER J. C. A. and SMITH D. (1996) Xenolith constraints on the thermal history of the mantle below the Colorado Plateau. *Geology* **24,** 267–270.

RODEN M. F., IRVING A. J., and MURTHY V. R. (1988) Isotopic and trace element composition of the upper mantle beneath a young continental rift: results from Kilbourne Hole, New Mexico. *Geochim. Cosmochim. Acta* **52,** 461–473.

RODEN M. F. and SHIMIZU N. (1993) Ion probe analyses bearing on the composition of the upper mantle beneath the Basin and Range and Colorado Plateau provinces. *J. Geophys. Res.* **98,** 14091–14108.

RYAN C. G., GRIFFIN W. L., and PEARSON N. J. (1996) Garnet Geotherms: a technique for derivation of P-T data from Cr-pyrope garnets. *J. Geophys. Res.* **101,** 5611–5625.

SCHULZE D. J. (1986) Calcium anomalies in the mantle and a subducted metaserpentinite origin for diamonds. *Nature* **319,** 483–485.

SCHULZE D. J. (1989) Constraints on the abundance of eclogite in the upper mantle. *J. Geophys. Res.* **94,** 4205–4212.

SEN G. (1987) Xenoliths associated with the Hawaiian hot spot. In *Mantle Xenoliths* (ed. P. H. NIXON). pp. 359–375. Wiley.

SEN G. (1988) Petrogenesis of spinel lherzolite and pyroxenite suite xenoliths from the Koolau shield, Oahu, Hawaii: implications for petrology of the post-eruptive lithosphere beneath Oahu. *Contrib. Mineral. Petrol.* **100,** 61–91.

SEN G. and LEEMAN W. P. (1991) Iron-rich lherzolitic xenoliths from Oahu: origin and implications for Hawaiian magma sources. *Earth Planet. Sci. Lett.* **102,** 45–57.

SIMMONS G. (1964) Velocity of compressional waves in various minerals at pressures to 10 kilobars *J. Geophys. Res.* **69,** 1117–1121.

SMITH D. (1979) Hydrous minerals and carbonates in peridotite inclusions from the Green Knobs and Buell Park kimberlitic diatremes on the Colorado Plateau. In *The mantle sample: Inclusions in kimberlites and other volcanics* (eds. F. R. BOYD and H. O. A. MEYER). pp. 345–356. Amer. Geophys. Union, Washington D.C.

SMITH D. and LEVY S. (1976) Petrology of the Green Knobs diatreme and implications for the upper mantle below the Colorado Plateau. *Earth Planet. Sci. Lett.* **29,** 107–125.

SMITH D. and BOYD F. R. (1987) Compositional heterogeneities in a high-temperature lherzolite nodule and implications for mantle processes, In *Mantle Xenoliths* (ed. P. H. NIXON). pp. 551–562. Wiley.

SMITH D., GRIFFIN W. L., RYAN C. G., COUSENS D. R., SIE S. H., and SUTER G. F. (1991) Trace-element zoning of garnets from The Thumb: a guide to mantle processes. *Contrib. Mineral. Petrol.* **107,** 60–79.

SMITH D., GRIFFIN W. L., and RYAN C. G (1993) Compositional evolution of high-temperature sheared lherzolite PHN1611. *Geochim. Cosmochim. Acta* **57,** 605–613.

SMITH D. and RITER J. C. (1997) Genesis and evolution of lower-Al orthopyroxene in spinel peridotite xenoliths, Grand Canyon field, Arizona, USA. *Contrib. Mineral. Petrol.* **127,** 391–404.

SMYTH J. R. and MCCORMICK T. C. (1995) Crystallographic data for minerals. In *Mineral physics and crystallography: a handbook of physical constants* (ed. T. J. AHRENS). pp. 1–17. Amer. Geophys. Union, Washington, D.C.

SOBOLEV N. V. (1977) *Deep-Seated Inclusions in Kimberlites and the Problem of the Composition of the Upper Mantle.* 279 pp. (English translation of Russian edition, 1974. Izdatel'stvo Mauka). American Geophysical Union, Washington, D.C.

SOBOLEV N. V., LAVRENT'EV YU. G., POKHILENKO N. P., and USOVA L. V. (1973) Chrome-rich garnets from the kimberlites of Yakutia and their parageneses. *Contrib. Mineral. Petrol.* **40,** 39–52.

SOBOLEV S. V., WIDMER R., and BABEYKO A. YU (1995) 3D temperature and composition in the upper mantle constraint by global seismic tomography and mineral physics. *Abst. 6th Intern. Kimberlite Conf.,* 561–563.

SONG Y. and FREY F. A. (1989) Geochemistry of peridotite xenoliths in basalt from Hannuoba, eastern China: implications for subcontinental mantle heterogeneity. *Geochim. Cosmochim. Acta* **53,** 97–113.

SPETSIUS Z. V. (1995) Occurrence of diamond in the mantle: a case study from the Siberian Platform. *J. Geochem. Explor.* **53,** 25–40.

SPETSIUS Z. V. and SERENCO V. P. (1990) *Composition of continental upper mantle and lower crust beneath the Siberian Platform.* Nauka.

STEIN M. and HOFMANN A. W (1992) Fossil plume head beneath the Arabian lithosphere. *Earth Planet. Sci. Lett.* **114,** 193–20..

STEIN M. and HOFMANN A. W. (1994) Mantle plumes and episodic crustal growth. *Nature* **372,** 63–68.

STOLZ A. J. and DAVIES G. R. (1988) Chemical and isotopic evidence from spinel lherzolite xenoliths for episodic metasomatism of the upper mantle beneath southeast Australia. *J. Petrol.* Special Lithosphere Issue, 303–330.

STOSCH H. -G. and LUGMAIR G. W. (1986) Trace element and Sr and Nd isotopic geochemistry of peridotite xenoliths from the Eifel (W. Germany) and their bearing on the evolution of the subcontinental lithosphere. *Earth Planet. Sci. Lett.* **80,** 281–298.

STOSCH H. G. and SECK H. A. (1980) Geochemistry and mineralogy of two spinel peridotite suites from Dreiser Weiher, West Germany. *Geochim. Cosmochim. Acta* **44,** 457–470.

STOSCH H. -G., LUGMAIR G. W., and KOVALENKO V. I. (1986) Spinel peridotite xenoliths from the Tariat depression, Mongolia. II: Geochemistry and Nd and Sr isotopic composition and their implications for the evolution of the subcontinental lithosphere. *Geochim. Cosmochim. Acta* **50,** 2601–2614.

SU W., WOODWARD R. L., and DZIEWONSKI A. M. (1994) Degree 12 model of shear velocity heterogeneity in the mantle. *J. Geophys. Res.* **99,** 6945–6980.

SUZUKI T. and AKOGI M. (1995) Element partitioning between olivine and silicate melt under high pressure. *Phys. Chem. Minerals* **22,** 411–418.

TANAKA T. and AOKI K. -I. (1981) Petrogenetic implications of REE and Ba data on mafic and ultramafic inclusions from Itinome-Gata. *Japan. J. Geology* **89,** 369–390.

UKHANOV A. V., RYABCHKOV I. D., and KHARKIV A. D. (1988) *Lithospheric mantle beneath the Yakutian kimberlite province.* Nauka. (in Russian).

VASELLI O., DOWNES H., THIRLWALL M., DOBOSI G., CORADOSSI N., SEGHEDI I., SZAKACS A., and VANNUCCI R. (1995a) Ultramafic Xenoliths in Plio-Pleistocene alkali basalts from the Eastern Transylvanian basin: depleted mantle enriched by vein metasomatism. *J. Petrol.* **36,** 25–53.

VASELLI O., DOWNES H., THIRLWALL M. F., VANNUCCI R., and CORADOSSI N. (1995b) Spinel-peridotite xenoliths from Kapfenstein (Graz Basin, Eastern Austria): a geochemical and petrological study. *Mineral. Petrol.* **57,** 23–30.

WALKER R. J., CARLSON, R. W., SHIREY S. B., and BOYD F. R. (1989) Os, Sr, ND and Pb isotope systematics of southern African peridotite xenoliths: implications for the chemical evolution of subcontinental mantle. *Geochim. Cosmochim. Acta* **53,** 1583–1595.

WALTER M. J. (1997) Melting of garnet peridotite and the origin of komatiite and depleted lithosphere. *J. Petrol* **39,** 29–60.

WIECHERT U., IONOV D. A., and WEDEPOHL K. H. (1996) Spinel peridotite xenoliths from the Atsagin-Dush volcano, Dariganga lava plateau, Mongolia: a record of partial melting and cryptic metasomatism in the upper mantle. *Contrib. Mineral Petrol.* **126,** 343–364.

WILKINSON J. F. G (1969) Ultramafic and associated rocks of north-eastern New South Wales. *J. Geol. Soc. Australia* **16,** 299–307.

WILKINSON J. F. G. (1975) Ultramafic inclusions and high pressure megacrysts from a nephelinite sill, Nandewar Mountains, north-eastern New South Wales, and their bearing on the origin of certain ultramafic inclusions in alkaline volcanic rocks. *Contrib. Mineral. Petrol.* **51,** 235–262.

WILSHIRE H. G. and BINNS R. A. (1961) Basic and ultrabasic xenoliths from the volcanic rocks of New South Wales. *J. Petrol.* **2,** 185–208

WILSHIRE H. G. and SHERVAIS J. W. (1975) Al-augite and Cr-diopside ultramafic xenoliths in basaltic rocks from western United States. *Phys. Chem. Earth* **9,** 257–272.

WITT-EICKSCHEN G. (1993) Upper mantle xenoliths from alkali basalts of the Vogelsberg, Germany: implications for mantle upwelling and metasomatism. *Europ. J. Mineral.* **5,** 361–376.

XU X., O'REILLY S. Y., GRIFFIN W. L., and ZHOU X. (1998) The nature of the Cenozoic lithosphere beneath Nushan, East Central China. In *Mantle dynamics and plate interactions in east Asia* (eds. M. F. J. FLOWER, S. L. CHUNG, C. H. LO, and T. Y. LEE) pp. 167–196. Geodynamics Vol. **27,** Amer. Geophys. Union, Washington, D.C.

YUAN X. (1996) Velocity structure of the Qinling lithosphere and mushroom cloud model, *Science in China* (Series D) **39,** 235–244.